

**Suppression of xylan endotransglycosylase PtXyn10A affects cellulose microfibril angle in secondary wall in aspen wood**

| | |
|-------------------------------|--|
| Journal: | <i>New Phytologist</i> |
| Manuscript ID: | NPH-MS-2014-17912.R1 |
| Manuscript Type: | MS - Regular Manuscript |
| Date Submitted by the Author: | n/a |
| Complete List of Authors: | <p>Debra-Maceluch, Marta; Swedish University of Agricultural Sciences, Department of Forest Genetics and Plant Physiology Awano, Tatsuya; Kyoto University, Division of Forest and Biomaterials Science Takahashi-Schmidt, Junko; Swedish University of Agricultural Sciences, Department of Forest Genetics and Plant Physiology Lucenius, Jessica; University of Helsinki, Department of Physics Ratke, Christine; Swedish University of Agricultural Sciences, Department of Forest Genetics and Plant Physiology; Swedish University of Agricultural Sciences, Department of Forest Genetics and Plant Physiology Kontro, Inkeri; University of Helsinki, Department of Physics Busse-Wicher, Marta; University of Cambridge, Department of Biochemistry Kosik, Ondrej; University of Cambridge, Department of Biochemistry Tanaka, Ryo; Kyoto University, Division of Forest and Biomaterials Science Winz ll, Anders; Royal Institute of Technology, School of Biotechnology Kallas,  sa; Royal Institute of Technology, School of Biotechnology Le niewska, Joanna; University of Białystok, Department of Botany Berthold, Fredrik; Innventia, Innventia AB Immerzeel, Peter; Swedish University of Agricultural Sciences, Department of Forest Genetics and Plant Physiology Teeri, Tuula; Aalto University, ; Royal Institute of Technology, School of Biotechnology Ezurra, Ines; Royal Institute of Technology, School of Biotechnology; KTH, Biotechnology Dupree, Paul; University of Cambridge, Department of Biochemistry Serimaa, Ritva; University of Helsinki, Department of Physics Mellerowicz, Ewa; Swedish University of Agricultural Sciences, Forest Genetics and Plant Physiology; Swedish University of Agricultural Sciences, Department of Forest Genetics and Plant Physiology</p> |
| Key Words: | Populus, hybrid aspen, secondary cell wall, wood formation, xylanase, xylan endotransglycosylase, cellulose microfibril angle, growth stresses |
| | |

For Peer Review

1 **Suppression of xylan **endo**transglycosylase *PtxtXyn10A* affects**
 2 **cellulose microfibril angle in secondary wall in aspen wood**

3
 4 Marta Derba-Maceluch^{1*}, Tatsuya Awano^{1,2*}, Junko Takahashi¹, Jessica Lucenius^{3,8},
 5 Christine Ratke¹, Inkeri Kontro³, Marta Busse-Wicher⁴, Ondrej Kosik^{4,9}, Ryo Tanaka²,
 6 Anders Winz ll⁵,  sa Kallas⁵, Joanna Le niewska^{1,6}, Fredrik Berthold⁷, Peter
 7 Immerzeel¹, Tuula T. Teeri^{5,10}, Ines Ezcurra⁵, Paul Dupree⁴, Ritva Serimaa³, and Ewa J.
 8 Mellerowicz^{1‡}

9 ¹ Department of Forest Genetics and Plant Physiology, SLU, Ume  Plant Science Centre
 10 (UPSC), Ume , Sweden

11 ² Division of Forest and Biomaterials Science, Graduate School of Agriculture, Kyoto
 12 University, Kyoto, Japan

13 ³ Department of Physics, University of Helsinki, PO Box 64, FIN-00014 Helsinki,
 14 Finland

15 ⁴ Department of Biochemistry, University of Cambridge, Tennis Court Road, CB2 1QW,
 16 Cambridge, UK

17 ⁵ School of Biotechnology, Royal Institute of Technology (KTH), Stockholm, Sweden

18 ⁶ Department of Botany, University of Białystok, Swierkowa 20 b, 15950 Białystok,
 19 Poland

20 ⁷ INNVENTIA AB, Drottning Kristinas v g 61, Stockholm, Sweden

21 ⁸ Present address: Aalto University, School of Chemical Technology, Department of
 22 Forest Products Technology, P.O. Box 16300, FI-00076 Aalto, Finland

23 ⁹ Present address: Centre for Crop Genetic Improvement, Department of Plant Biology
 24 and Crop Science, Rothamsted Research, West Common, Harpenden, Herts AL5 2JQ,
 25 UK

26 ¹⁰ Present address: Aalto University, P.O.Box 17800, FI-00076 Aalto, Finland

27 * These authors contributed equally to this work.

28

29 ‡**Author for correspondence**

30 Ewa J. Mellerowicz

31 **Tel:** +46 90 786 8367

32 **Email:** ewa.mellerowicz@slu.se

33

34 Introduction: 651 words.

35 Materials and Methods: 1974

36 Results: 2659

37 Discussion: 1184

38 Acknowledgements: 68

39

40 Figures 1 – 9. Figures 1, 5 and 9 should be published in colour.

41 Tables 1 – 2.

42 Supporting Information : Fig. S1 – S6, Method S1, Tables S1 – S6.

43

44 Financial sources: Formas (including HemiPop and FuncFiber), Swedish Research
45 Council (VR), Swedish Governmental Agency for Innovation Systems (VINNOVA),
46 Swedish Center for Biomimetic Fiber Engineering (funded by the Knut & Alice
47 Wallenberg Foundation and the Foundation for Strategic Research), European projects
48 EDEN (QLK5-CT-2001-00443) and RENEWALL, FORE, Bio4Energy, Wood
49 Ultrastructure Research Centre, SamNordisk Skogsforskning (project no. 107), Japan
50 Society for the Promotion of Science (JSPS KAKENHI Grant Number 24580243) and
51 the Academy of Finland (1127759).

52

53 Summary

- 54 • Certain xylanases from family GH10 are highly expressed during secondary wall
55 deposition, but their function is unknown. We carried out functional analyses of
56 the secondary-wall specific *PtxtXyn10A* in hybrid aspen (*Populus tremula* L. x
57 *tremuloides* Michx.).
- 58 • *PtxtXyn10A* function was analysed by expression studies, overexpression in
59 Arabidopsis protoplasts and by downregulation in aspen.
- 60 • *PtxtXyn10A* overexpression in Arabidopsis protoplasts resulted in increased
61 xylan **endotransglycosylation rather than hydrolysis**. In aspen, the enzyme was
62 found to be proteolytically processed **to a 68 kDa peptide and residing in cell**
63 **wall. Its downregulation** resulted in a corresponding decrease in xylan
64 **endotransglycosylase** activity and no change in xylanase activity. This did not
65 alter xylan molecular weight or its branching pattern but affected the cellulose-
66 microfibril angle in wood fibres, increased primary growth (stem elongation, leaf
67 formation and enlargement) and reduced the tendency to form tension wood.
68 Transcriptomes of transgenic plants showed downregulation of tension wood
69 related genes and changes in stress-responsive genes.
- 70 • The data indicate that *PtxtXyn10A* acts as a xylan **endotransglycosylase** and its
71 main function is to release tensional stresses arising during secondary wall
72 deposition. **Furthermore, they suggest that regulation of stresses in secondary**
73 **walls plays a vital role in plant development.**

74
75 **Key words:** *Populus*, hybrid aspen, secondary cell wall, wood formation, xylanase, xylan
76 **endotransglycosylase**, cellulose microfibril angle, growth stresses

77

78 **Introduction**

79 Xylans are **among most abundant** polysaccharides found in nature (Ebringerová &
80 Heinze, 2000; Scheller & Ulvskov, 2010). They are polymers with a β -1,4-D-
81 xylopyranose backbone and include homoxylans and heteroxylans, such as
82 arabinoxylans, glucuronoxylans and glucuronoarabinoxylans. Glucuronoxylans are
83 abundant in the secondary walls of dicotyledonous species, where they are the main
84 hemicellulose, comprising roughly one fourth of wood biomass, whereas arabinoxylans
85 and glucuronoarabinoxylans are found in type II primary cell walls of grasses and
86 secondary walls of conifers, respectively. Small amounts of glucuronoarabinoxylans are
87 also present in the primary cell walls of eudicots and lower vascular plants (Darvill *et al.*,
88 1980; McCartney *et al.*, 2006; Brummell & Schröder, 2009). The importance of
89 understanding the biosynthesis and modification of xylans in plants is emphasised by the
90 increasing significance of plant biomass as a potential source of renewable energy and
91 use of hemicelluloses as food additives and pharmacologically active ingredients (Bevan
92 & Franssen, 2006).

93 In *Populus* wood, xylans have a backbone of approximately 100 units long with side
94 chains of 4-*O*-methyl- α -D-glucuronic acid (Me-GlcUA) at *O*-2 in approximately every
95 tenth xylose residue (Timell, 1967; Teleman *et al.*, 2000). In addition, approximately
96 50% of the xylose residues are *O*-acetylated at the C-2, C-3 or both positions (Naran *et*
97 *al.*, 2009). An oligosaccharide containing β -D-Xyl-(1,4)- β -D-Xyl-(1,3)- α -L-Rha-(1,2)- α -
98 D-GalUA-(1,4)-D-Xyl resides at the reducing end of the *Populus* xylan, similar to found
99 in other eudicots and conifers (Lee *et al.*, 2011). In secondary walls, glucuronoxylans are
100 thought to interact with lignin via ester bonding to GlcUA and Me-GlcUA (Imamura *et*
101 *al.*, 1994; Spániková & Biely, 2006; Spániková *et al.*, 2007; Li *et al.*, 2007).

102 The biosynthesis of xylan involves several different classes of glycosyltransferases (GTs)
103 that make up the backbone, the reducing end sequence and different side chains (recently
104 reviewed by Rennie & Scheller, 2014). These enzymes reside in the Golgi apparatus,
105 where they probably form synthesising complexes along with other enzymes involved in
106 the methylation of glucuronate side chains and acetylation of the backbone. The

107 preformed xylan is deposited in the cell wall, where it associates with cellulose
108 microfibrils by hydrogen bonding (Kabel *et al.*, 2007; Busse-Wicher *et al.*, 2014) and
109 may traverse several wall layers or be modified *in muro*, resulting in xylan epitope
110 accumulation in the outer wall layers (Awano *et al.*, 2002). Different types of xylan-
111 acting enzymes are known to reside in plant cell walls: endo-1,4- β -xylanase (EC 3.2.1.8),
112 xylan endotransglycosylase (also known as trans- β -xylanase), 1,4- β -xylosidase (EC
113 3.2.1.37) and bifunctional α -arabinofuranosidase/ β -xylosidase (Goujon *et al.*, 2003; Fry,
114 2004; Minic & Jouanin, 2006; Ichinose *et al.*, 2010; Franková & Fry, 2011; 2013;
115 Johnston *et al.*, 2013).

116 Plant endo-1,4- β -xylanases belong to the glycoside hydrolase family 10 (GH10) and
117 appear to be involved in xylan modification in primary and secondary walls, but their
118 function is only understood for tissues undergoing decomposition involving digestion of
119 cell wall xylan (Paull & Chen, 1983; Benjavongkulchai & Spencer, 1986; Slade *et al.*,
120 1989; Banik *et al.*, 1996; Cleemput *et al.*, 1997a, b; Bih *et al.*, 1999; Wu *et al.*, 2002;
121 Simpson *et al.*, 2003; Chen & Paull, 2003; Suen & Huang, 2006). GH10 enzymes are
122 also known to be highly expressed in xylem, but their function in this tissue is not yet
123 clear (Mellerowicz *et al.*, 2001; Suzuki *et al.*, 2002; Geisler-Lee *et al.*, 2006). One of
124 these genes, *PtxtXyn10A*, which shows high similarity to *AtXyn1* (Suzuki *et al.*, 2002),
125 has been found to be upregulated during xylem secondary cell wall formation in hybrid
126 aspen (*Populus tremula* L. x *tremuloides* Michx.) (Hertzberg *et al.*, 2001; Aspeborg *et al.*,
127 2005). Therefore, to investigate its function during xylogenesis, we analysed its
128 activity, expression and effects of its suppression in hybrid aspen. We found that
129 *PtxtXyn10A* acts mainly as a xylan endotransglycosylase and affects the cellulose
130 microfibril angle (MFA) and other aspects of plant development. Based on our data, we
131 propose that the main function of Xyn10A in secondary walls is to release mechanical
132 stress arising during cell wall deposition.

133

134 **Materials and Methods**

135 ***Cloning of full length PtxtXyn10A***

136 A partial clone of *PtxtXyn10A* was identified among the EST clones from a cambial
137 region cDNA library of hybrid aspen (Sterky *et al.*, 2004). 5' RACE was carried out and
138 full-length clones were obtained, cloned into the pGEM-T Easy vector (Promega, USA)
139 and sequenced. The cDNA GenBank accession number is AY935501.

140 ***Plant material and growth conditions***

141 Hybrid aspen, *Populus tremula* L. x *tremuloides* Michx., trees (clone T89) were grown in
142 a greenhouse with a long photoperiod as described previously (Gray-Mitsumune *et al.*,
143 2008) until they reached approximately 2 m in height.

144 ***RT-qPCR analysis***

145 One µg of total DNA-free RNA isolated from the primary- and secondary-walled
146 developing xylem or transformed *A. thaliana* protoplasts was used for reverse
147 transcription using an iScript™ cDNA biosynthesis kit (Bio-Rad). Primers (Table S5)
148 were designed using QuantPrime (<http://www.quantprime.de>) and Primer3Web 0.4.0
149 (<http://primer3.sourceforge.net>). The best reference gene (CYP in aspen and EF1a and
150 UBQ5 in *Arabidopsis*) was selected using GeNorm (<http://www.bigazelle.com>;
151 Vandesompele *et al.*, 2002) among ADF6, actin, UBQ CYP, EiF1a, clatrin and APT. An
152 iQ™ SYBR Green Supermix (BioRad) kit was used and Cq values were acquired using a
153 Light Cycler 480 1.5.0.sp3 (Roche). Relative expression was calculated as $E_T^{(Cq1-Cq2)}/E_R^{(Cq1-Cq2)}$
154 in aspen (where E_T and E_R are the efficiencies of the target and reference genes,
155 respectively, and Cq1 and Cq2 are the Cq levels for the sample and control, respectively)
156 or as $2^{-\Delta\Delta Cq}$ (Livak *et al.*, 2001) in *Arabidopsis*.

157 ***Immunoblotting***

158 For the production of polyclonal antibody Kamisa detecting *PtxtXyn10A*, a cDNA
159 fragment from the clone A020P21 (accession number AI162606) encoding a C-terminal
160 *PtxtXyn10A* fragment was cloned into pAFF8c-3c (Larsson *et al.*, 2000). The
161 recombinant protein was produced in *E. coli* and purified using TALON® protein

162 purification columns (Clontech, USA). The purified 66 kDa soluble recombinant protein
163 was used as antigen. For the production of antibody Abbe against the *PtxtCel9B3* protein,
164 a protein based on the full-length cDNA clone (accession number AY660968) was used
165 in a similar fashion. The polyclonal antibodies were produced in rabbits by Agrisera AB,
166 Sweden.

167 Soluble proteins were extracted according to Biswal *et al.* (2014), and cell wall bound
168 proteins were extracted from the remaining pellet by incubation in Laemmli buffer (10%
169 (v/v) glycerol, 5% (v/v) 2-mercaptoethanol, 2% (w/v) SDS, 62.5 mM Tris-HCl, pH 6.8)
170 at 100°C for 10 min. The suspension was cooled to room temperature, subjected to
171 centrifugation at 15000 g for 20 min, then 30 µg of each protein sample was loaded onto
172 a NuPage® Novex Bis-Tris gel (Invitrogen, USA) and blotted onto a nitrocellulose
173 membrane. The membrane was probed overnight at 4°C with a 1:1000 dilution of Kamisa
174 antibody. Signals were revealed using the Amersham ECL System. The same membrane
175 was subsequently probed with the antibody Abbe raised against a cell wall bound
176 cellulase *PtxtCel9B3* (Takahashi *et al.*, 2009).

177 ***Intracellular localization of PtxtXyn10A***

178 *PtxtXyn10A* cDNA was subcloned into the binary vector pEarleyGate103 using the
179 primers listed in Table S6. *Arabidopsis* was transformed using the floral dip method
180 (Clough & Bent, 1998). Detection of recombinant protein was carried out as previously
181 described (Latha Gandla *et al.*, 2014; Pawar PAM *et al.*, in revision).

182 ***Detection of endoxylanase and xylan endotransglycosylase activities in plants***

183 ***Protein extraction.*** Secondary-walled developing xylem from transgenic and WT (T89)
184 hybrid aspen was scraped and ground in liquid nitrogen. Soluble and wall-bound proteins
185 were isolated as previously described (Biswal *et al.*, 2014). All buffers contained
186 complete protease inhibitor cocktail (Roche). Transfected *Arabidopsis* protoplasts were
187 harvested by centrifugation and proteins were extracted using buffer comprising 0.1 M
188 Na succinate (pH=4.7) and 10 mM CaCl₂.

189 ***Thin-layer chromatography for detecting products of xylanase and xylan***

190 ***endotransglycosylase activities.*** Protein extracts containing either 1.25 mM or 6.25 mM

191 Xylo₆ (Megazyme, Ireland) were incubated at 40°C for 48 h. Volumes corresponding to
192 the same amounts of substrates were analysed on TLC Silica Gel 60 Glass plates as
193 described by Franková & Fry (2011).

194 **Quantitative analysis of xylan *endo*transglycosylase using a fluorogenic substrate.** To
195 prepare the fluorogenic substrate, 20 µg of Xylo₆ (Megazyme, Ireland) was labelled with
196 8-aminonaphthalene-1, 3, 6-trisulfonic acid (ANTS, Invitrogen) according to (Kosik *et al.*
197 (2012). The NaCNBH₃ was quenched with a two-fold molar excess of hydrochloric acid,
198 re-neutralised with NaOH to pH 7, dried in vacuum and re-dissolved in a small amount of
199 MilliQ water. The solution containing Xylo₆-ANTS was then spotted onto a dry column
200 packed with Silicagel 60 (Merck, Germany). The excess ANTS was washed out with *iso*-
201 propanol:NH₄OH:water (5:1:1, v/v/v) and 0.5 mL flow-through fractions were collected
202 and dried down. Xylo₆-ANTS was eluted off the column with 40% ethanol (v/v), dried
203 down in vacuum, reconstituted in a small amount of 3 M urea and electrophoresed on a
204 PACE gel together with the flow through fractions to ensure the purity of the product.
205 The concentration of Xylo₆-ANTS was estimated from absorbance measured at 365 nm
206 and calculated using a calibration curve.

207 An *endo*transglycosylation assay was performed according to Kosik *et al.* (2011) with the
208 following modifications: extracted proteins were incubated in 0.15% birch xylan (Sigma)
209 and 165 µM Xylo₆-ANTS at RT for 1 h. Reactions were loaded onto circles of Whatman
210 3MM chromatographic paper in ELISA UV plates, then washed and the bound
211 fluorescence measured using a Spectra Max Gemini (Molecular Devices) micro-plate
212 reader at 355 nm excitation and 538 nm emission. For the blank samples, reactions
213 without Xylo₆-ANTS were used. Product bound to 3MM paper was treated with 1 U of
214 either *endo*-1,4-β-xylanase M1 from *T. viride* (Megazyme) or pectate lyase from *C.*
215 *japonicus* (Megazyme) **used as an example of xylan-inert enzyme** in extraction buffer or
216 in the extraction buffer only, for 1 h at 40°C. The reaction was stopped by washing three
217 times with 66% ethanol. Fluorescence of the remaining product was measured as above.

218 **Xylanase activity.** Azo-Xylan (from birchwood, Megazyme) was used for the
219 measurement of endoxylanase activity. The reaction was performed according to the
220 manufacturer's instructions for 20 h at 40°C in 0.1 M succinate buffer, pH 5.5. β-

221 xylanase M1 from *Trichoderma viride* (Megazyme) was used to construct the standard
222 curve.

223 To quantify hydrolytic activity by reducing ends, 0.25% (w/v) birchwood xylan (Sigma)
224 was incubated with extracted proteins in 0.1 M Na-succinate buffer, pH 5.5 at 40°C for
225 20 h. The reaction was stopped by boiling for 5 min in PAHBAH reagent (1.5% *p*-
226 hydroxybenzoic acid hydrazide in 0.5 M NaOH) and absorbance was measured at 410 nm
227 after cooling (Lever, 1972). Xylose (2 mM to 0.0078 mM) was used to construct the
228 standard curve and the data were calibrated to units of β -xylanase M1 from *Trichoderma*
229 *viride* (Megazyme).

230 ***Expression of PtxtXyn10A in Arabidopsis cells***

231 Full length *PtxtXyn10A* cDNA was amplified (primers listed in Table S6). The products
232 were cloned into the pENTR/D-TOPO vector (pENTR™ Directional TOPO® Cloning
233 Kits, Invitrogen), sequenced and subsequently subcloned into the binary vector
234 pK2WG7.0 (Karimi *et al.*, 2002) using the Gateway® system (Invitrogen).

235 An *Arabidopsis* cell suspension derived from roots was used for protoplast isolation and
236 transient protoplast transformations according to Dóczi *et al.* (2011) with slight
237 modifications: 5×10^5 protoplasts were used for each transformation with 5 μ g of plasmid
238 DNA without any carrier. After transformation, protoplasts were incubated in the dark for
239 24 h and harvested by centrifugation at 300 g for 8 minutes.

240 ***Generation of transgenic antisense aspen***

241 For the antisense construct, cDNAs of C-terminal fragments covering the whole catalytic
242 module of *PtxtXyn10A* and 28 bp of the 3' end of CBM22_3_{*PtxtXyn10A*} were amplified,
243 cloned into the binary vector pPCV702.kana and transferred to hybrid aspen as described
244 previously (Gray-Mitsumune *et al.*, 2008) using *Agrobacterium tumefaciens*.

245 ***FT-IR spectroscopic analysis***

246 Wood at internode 44 from five to seven trees of selected lines and the WT were
247 individually examined as previously described (Latha Gandla *et al.*, 2014). The initial
248 PCA analysis was carried out with 28 observations and 624 variables on UV scaled pre-

249 treated spectra. After excluding outliers, OPLS-DA analyses (Trygg & Wold, 2002) were
250 performed to identify wavenumbers that distinguished different classes based on cell wall
251 composition. The OPLS-DA model was based on 21 observations and approximately 624
252 variables from Pareto-scaled pre-treated spectra using two classes (WT and transgenic).

253 ***Physicochemical wood analyses***

254 Transgenic antisense lines carrying the antisense *PtxtXyn10A* construct (lines 2, 3 and 32)
255 and a WT line (clone T89) were each represented by a minimum of 5 trees. Basal
256 internodes from trees approximately 2 m tall, taken below internode 46, were frozen in
257 liquid N and stored at -80°C. The samples were thawed, debarked, hand chipped and
258 dried before analysis.

259 ***Wet chemistry of wood.*** Bulk wood samples were analysed for lignin content and
260 carbohydrate composition as described in method AH 23-18 (Theander & Westerlund,
261 1986). The method involves full hydrolysis of samples, followed by derivatisation of
262 liberated monomers and gas chromatography. Lignin content (Klason and acid soluble)
263 was determined according to SCAN-C.1. The hemicellulose molecular weight was
264 determined using size-exclusion chromatography (SEC) according to Jacobs & Dahlman
265 (2001). Hemicellulose was isolated by extraction using 24% w/v KOH after
266 delignification of samples using chlorite and fractionated using hydrogel columns (120,
267 250, 500). An alkaline solution containing 0.2 M NaOH and 0.1 M acetate was used as
268 eluent. The molecular weight was calculated based on standard curves obtained from
269 fractionation and MALDI-TOF measurements (Jacobs & Dahlman, 2001).

270 The glucuronoxylan branching pattern was determined by PACE using
271 glucuronoxylanase GH30 as described in Bromley *et al.* (2013). Briefly, wood powder
272 was treated with 4 M NaOH, then neutralized with HCl, buffered with 0.1 M ammonium
273 acetate pH 6.0 and digested with glucuronoxylanase (*BoGH30*; Bacova_03432,
274 Rogowski *et al.*, 2014) for 2 h at room temperature. Digestion products, along with no
275 enzyme and enzyme only controls, were labelled with ANTS, separated by
276 polyacrylamide gel electrophoresis as described in Goubet *et al.* (2002) and visualised
277 with a G-box UV gel documentation system (Syngene).

278 **X-ray diffraction.** Aspen stem segments without bark and pith were divided into three
279 classes according to xylem thickness. Four replicates from the WT and three replicates
280 from each of the transgenic antisense lines were measured in each size class after drying
281 at 300 K. The X-ray diffraction experiments and data analysis for the determination of
282 cellulose crystallite size, microfibril angle distribution and crystallinity index were
283 conducted using $\text{CuK}\alpha_1$ radiation (1.54 Å) as explained in Svedström *et al.* (2012).

284 ***Slit pit angle***

285 Wood from internodes 42-43 was macerated as previously described (Gray-Mitsumune *et*
286 *al.*, 2008). Cells were examined under an Axioplan 2 microscope (Zeiss). To measure the
287 cellulose microfibril angle, the angle of slit pits was measured in three to five pits for
288 each fibre, and at least 50 fibres were measured for each of three randomly selected trees
289 per line.

290 ***Field-emission scanning electron microscopy***

291 FAA-fixed stem segments from internode 30 were washed with water and sectioned to
292 small cubes with a cryomicrotome (Microm HM 505E), treated with 0.1% (v/v) sodium
293 hypochlorite for three min and dehydrated in an ethanol series prior to critical point
294 drying. The specimens were mounted on an aluminium stub and coated with 5 nm
295 iridium. For imaging, a Zeiss Merlin field emission SEM was used with 4 kV
296 accelerating voltage.

297 ***Microarray analysis***

298 RNA and array preparation was carried out according to UPSC-BASE standardized
299 procedures (Sjödín *et al.*, 2006). The different scan levels for each slide were merged
300 using restricted linear scaling (RLS) followed by step-wise normalization before further
301 analysis. B-statistics were calculated against line 2 and 32 and the two lists of array
302 elements were compared. Genes in antisense lines were considered differentially
303 regulated if $B \geq 0$ and $P \leq 0.05$ compared to a reference WT. Genes selected from the
304 ranking list of B-statistics were annotated against the *Populus* genome (Phytozome 9.0).

305 ***Statistical analysis***

306 Univariate data were subjected to analysis of variance followed by post-hoc tests as
307 indicated using the JMP 7 program (SAS Inc., USA). Multivariate data analysis was
308 performed using SIMCA-P software (version 11.0.0.0, Umetrics AB, Sweden).

309

310 **Results**

311 ***Molecular cloning and bioinformatic analysis of PtXyn10A***

312 The full-length *PtxtXyn10A* cDNA sequence was cloned from a cDNA library of
313 developing xylem in hybrid aspen (GenBank accession number AY935501). The
314 predicted *PtxtXyn10A* peptide lacks a signal sequence and contains three carbohydrate-
315 binding modules family 22 (CBM22) followed by a Xyn10 catalytic domain (Fig. 1a).
316 Five *N*-glycosylation sites and one processing site after R-329, releasing the mature
317 peptide with molecular weight 65.3 kDa and pI = 5.77, were predicted by the sequence
318 analysis.

319 ***Populus GH10 gene family***

320 The *Populus trichocarpa* genome contains eight GH10 genes, *i.e.* *PtXyn10A* - *PtXyn10H*,
321 of which seven have been previously identified (Geisler-Lee *et al.*, 2006) and one,
322 *PtXyn10H*, was found in the region directly upstream of *PtXyn10A* on chromosome 2
323 (Fig. S1; Table S1). *PtXyn10A* and *PtXyn10H* have been merged into one model in the
324 current version of Phytozome (9.1), but our rapid amplification of cDNA ends (RACE)
325 and polymerase chain reaction (PCR) experiments confirmed the existence of two loci
326 (Fig. S1; Table S1).

327 *PtXyn10B* lacks part of the catalytic domain and a corresponding truncated gene is also
328 found in *Arabidopsis thaliana*. Phylogenetic analysis of the remaining genes of *P.*
329 *trichocarpa* and *A. thaliana* (Henrissat *et al.*, 2001) has revealed four well-defined clades
330 with members in both species (Fig. S2). The clade to which *PtXyn10A* belongs, together
331 with its closest paralog *PtXyn10H* and four *Arabidopsis* genes, including *AtXyn1*, is
332 characterised by the presence of 2-4 CBMs. Other clades include genes with one CBM or
333 none.

334 ***Xyn10A is the main GH10 transcript in secondary-walled developing xylem***

335 Reverse transcription-PCR (RT-PCR) revealed a high abundance of *PtxtXyn10A*
336 transcripts in stems and roots with secondary growth and low abundance in the apical bud
337 and mature leaves (Fig. S3a), consistent with its localisation to developing secondary-
338 walled xylem seen in microarray studies (Hertzberg *et al.*, 2001; Aspeborg *et al.*, 2005).

339 To determine in which xylem cell types *PtxtXyn10A* is expressed, we performed *in situ*
340 RT-PCR in stem sections using gene-specific nested primers (Gray-Mitsumune *et al.*,
341 2004). *Xyn10A*-specific signals were detected in all cell types in developing wood, fibres,
342 vessel elements and ray cells, with the highest expression observed during the early
343 stages of secondary wall deposition (Fig. S3b).

344 To compare the expression pattern of *Xyn10A* in wood-forming tissues to that of other
345 *Populus* GH10 family members, we examined the relative transcript abundance of GH10
346 genes in cambium/phloem versus secondary wall developing xylem by RT-qPCR.

347 Transcripts of *Xyn10A*, *Xyn10D*, *Xyn10E* and *Xyn10G* were detected in developing
348 xylem, but only *Xyn10A* was highly upregulated in the secondary wall forming xylem
349 (Fig. S4a). Moreover, based on *Populus* microarray data (<http://bar.utoronto.ca/>; Wilkins
350 *et al.*, 2009), the expression levels of other GH10 genes were found to be several orders
351 of magnitude lower than those of *Xyn10A* in developing wood (Fig. S4b).

352 ***Xyn10A protein is present in xylem cell walls as a 68 kDa peptide***

353 To detect the Xyn10A protein in wood-forming tissues, the polyclonal antibody named
354 “Kamisa” was raised against the C-terminal part of the *PtxtXyn10A* peptide. Soluble
355 proteins were removed from crude plant extracts using a low ionic strength buffer, and
356 proteins bound to the remaining pellet, including cell wall bound proteins, were extracted
357 with a sodium dodecyl sulphate (SDS) containing buffer. A clear band at approximately
358 68 kDa was detected in the cell wall fraction from developing xylem consistent with the
359 expected processed 65 kDa protein together with predicted glycosylations (Fig. 1b). No
360 signal was detected in the soluble fraction from this tissue or in any fraction from the
361 apical bud tissues in which the gene was lowly expressed (Fig. S3a).

362 Although *PtxtXyn10A* lacks a predicted signal peptide (Table S1), the SecretomeP 2.0
363 server (<http://www.cbs.dtu.dk/services/SecretomeP/>) predicted its target to be the
364 apoplasm. To verify the cellular localization experimentally, a 35S::*PtxtXyn10A*:eGFP
365 construct was expressed in Arabidopsis. The GFP signal was detected in cell walls, but it
366 was weak and labile, probably due to the acidic pH of cell walls. However, the fusion
367 protein was clearly immunolocalised in cell walls after protoplast plasmolysis (Fig. 1c).

368 *Aspen xylem wall-bound proteins exhibit xylan endotransglycosylase and xylanase*
369 *activities in a substrate concentration-dependent manner*

370 Both xylanase and xylan endotransglycosylase activities have been detected in plant
371 tissues, latter activity requiring higher substrate concentration (Franková & Fry, 2011;
372 Johnston *et al.*, 2013). A similar dependence of activity on substrate concentration is also
373 known for microbial GH10 enzymes (Charnock *et al.*, 1997). Therefore, we investigated
374 if such activities could be detected in proteins extracted with high ionic strength buffer
375 from developing xylem (where *PtxtXyn10A* is expressed as the main GH10 enzyme)
376 when using xylohexaose as substrate. Under these conditions, it was expected that
377 hydrolytic activity would yield products with DP 1-5, whereas endotransglycosylase
378 activity would give a mixture of products with larger and lower DP than 6. When 1.85
379 mM xylohexaose was incubated with aspen protein extracts, products with DP 1 to DP 5
380 accumulated in a time-dependent manner, indicative of hydrolysis (Fig. 2a). However,
381 when the concentration of xylohexaose was increased to 4 mM (data not shown) or 6.125
382 mM, products with DP values ranging from 8 to 10 were additionally detected, indicative
383 of endotransglycosylation (Fig. 2a). The main products had DP 9 and DP 3,
384 corresponding to cleavage in the middle of xylohexaose followed by transglycosylation.
385 This shows that developing xylem cells exhibit xylan hydrolase and xylan
386 endotransglycosylase activities and that the endotransglycosylase activity requires a
387 higher substrate concentration than hydrolase (> 1.85 mM xylohexaose in the present
388 experimental setup).

389 To establish a quantitative assay for xylan endotransglycosylation in high ionic strength
390 protein extracts of developing wood, the extracts were incubated with birchwood xylan

391 (the donor) and 8-aminonaphtalene-1,3,6-trisulfonic acid-labelled Xylo6 (Xylo6-ANTS;
 392 the acceptor). Xylan **endotransglycosylation resulted in** a high molecular weight ANTS
 393 labelled product, which was bound to cellulose and detected by fluorimetry (Fig. 2b).
 394 This product was significantly more susceptible to xylanase M1 than to pectate lyase or
 395 reaction buffer, confirming that it was xylan-labelled with ANTS (Fig. 2c). Decreased
 396 fluorescence observed after incubation in the buffer at 40°C was attributed to the
 397 instability of ANTS.

398 ***PtxtXyn10A* expression in Arabidopsis cells strongly increases xylan**
 399 ***endotransglycosylation but not xylan hydrolysis***

400 To investigate which activity (xylan hydrolase or xylan **endo**transglycosylase) was
 401 encoded by *PtxtXyn10A*, *Arabidopsis* protoplasts were transfected by either *PtxtXyn10A*
 402 or an empty vector and proteins were extracted from the samples expressing the
 403 transgenes, as verified by RT-qPCR. Xylan **endo**transglycosylation detected by ANTS
 404 assay was significantly increased in cells expressing *PtxtXyn10A* compared to the empty
 405 vector control (Fig. 3a).

406 The same samples were tested for xylanase activity using either the *endo*-1,4- β -xylanase
 407 assay measuring solubilisation of AZO-xylan or the reducing end assay. Weak xylanase
 408 activity (four orders of magnitude lower than that of M1 xylanase from *Trichoderma*
 409 *viride* used for normalisation) was detected by these two assays in extracts for the empty
 410 vector and *PtxtXyn10A* expressing cells, and no significant differences between these
 411 extracts were detected (Fig. 3b and c). These results indicate that *PtxtXyn10A*-encoded
 412 enzyme exhibits xylan **endo**transglycosylase rather than xylanase activity *in vitro*.

413 ***Suppression of PtxtXyn10A* expression in transgenic aspen**

414 To study the physiological role of *PtxtXyn10A*, ten transgenic antisense lines of hybrid
 415 aspen were generated and two or three most highly affected antisense lines were selected
 416 for subsequent analyses. *PtxtXyn10A* transcript levels were decreased to approx. 50% of
 417 the WT level in the selected lines (Fig. 4a) and western blotting using Kamisa antibody
 418 showed a corresponding reduction of *PtxtXyn10A* protein in extracts obtained from
 419 xylem with high ionic strength buffer (Fig. 4b). The xylan **endo**transglycosylation by

420 these extracts was significantly lower in transgenic antisense lines compared to WT (Fig.
421 4c), but the xylanase activity was not affected (Fig. 4 d). These data indicate that the
422 suppression of *PtxtXyn10A* affects xylan **endo**transglycosylase but not xylanase activity
423 in developing wood.

424 The transgenic antisense lines exhibited increased growth in height, internode number
425 and leaf size (Fig. 5). Stem diameters and petiole lengths were also recorded, but no clear
426 changes were detected for these variables. To investigate if the increased growth was
427 caused by a change in the primary cell wall plasticity, thereby affecting cell size, casts
428 were prepared from the adaxial leaf epidermis and the cell surface area was determined
429 by microscopy. No significant difference in cell surface area between the transgenic
430 antisense lines and WT was found (Fig. 5). Thus, *PtxtXyn10A* suppression does not
431 increase leaf growth by increasing primary wall plasticity but by stimulating cell division.

432 ***Effects of PtxtXyn10A on xylan structure***

433 The two putative activities of *PtxtXyn10A* were expected to differentially affect xylan
434 chain length: xylanase would decrease it, whereas xylan **endo**transglycosylase may
435 increase, decrease or not affect it depending on the length of input acceptor; without any
436 input, the average length of xylan should not be altered by **endo**transglycosylation. Size
437 exclusion chromatography of a 24% (w/v) KOH-extracted hemicellulose fraction
438 containing mainly glucuronoxylan (Jacobs & Dahlman, 2001) gave similar weight-
439 averaged molecular weights (M_w) for WT (15 600) and transgenic antisense lines (15 100
440 to 15 500); the polydispersity index (M_w/M_n) ranged between 1.13 and 1.14 for all the
441 lines (Table S2). Thus, no major change in glucuronoxylan molecular weight was
442 detected, consistent with *PtxtXyn10A* acting as an **endo**transglycosylase *in vivo*.

443 To determine if the (Me)GlcA branching pattern of glucuronoxylan was affected by the
444 **endo**transglycosylase activity, we used glucuronoxylanase *BoGH30*, which acts
445 specifically on the xylan backbone and cleaves only when it is substituted with (Me)GlcA
446 at the -2 position. The lengths of the digestion products thus corresponded to intervals of
447 (Me)GlcA substitutions on the xylan backbone. PACE analysis of the labelled digestion
448 products gave similar profiles for the transgenic antisense lines and WT aspen (Fig. 6).

449 The detected bands agreed with those previously described in *Arabidopsis xylan*
450 (Bromley *et al.*, 2013) and corresponded to oligosaccharides arising from two xylan
451 domains: evenly spaced longer (DP 6 to DP over 20) oligosaccharides of the major
452 domain and shorter (DP 5 to 7), odd or even length fragments derived from the minor
453 domain. The presence of both types of products in all examined lines indicates that both
454 xylan domains are present in aspen wood and are not affected by the xylan
455 **endo**transglycosylase activity.

456 ***Effects of PtxtXyn10A on wood cell wall composition***

457 To determine whether reduced xylan **endo**transglycosylase activity affects other polymers
458 in cell wall, diffuse reflectance Fourier-transformed infrared (FT-IR) spectra of milled
459 wood of transgenic and WT plants were analysed. Orthogonal projections to latent
460 structure discriminant analysis (OPLS-DA) showed separation of the transgenic and WT
461 spectra, indicating alterations in cell wall composition (Fig. 7 a). Among the bands
462 contributing to the separation, there were several vibrations corresponding to different
463 forms of lignin. The 1460 cm⁻¹ band (C-H deformation/bending in aromatics; Dokken *et*
464 *al.*, 2005) and 1506/1595 band ratio, which reflects the condensed and cross-linked lignin
465 structure (Akin *et al.*, 1993; Stewart *et al.*, 1997), were increased in the transgenic lines
466 (Fig. 7 b). The ratio of absorbance at 1506 cm⁻¹ to that at 900 cm⁻¹ (representing the
467 anomeric C-O stretch in cellulose (Zhong *et al.*, 2000)) was significantly higher in the
468 transgenic lines, suggesting that they may have more lignin relative to cellulose. The
469 observation that the entire spectral region between 1000–1100 cm⁻¹ (sugar-ring
470 vibrations) was more intense in the WT also indicates a higher lignin to cellulose ratio in
471 the transgenic lines as the corresponding carbohydrates were less likely to be
472 hemicelluloses or pectins because their intensity negatively correlated with that of the
473 1730 cm⁻¹ –C=O vibration (Fig. 7 b).

474 To support these conclusions, we performed wet chemical analyses on wood material
475 from the transgenic lines and WT. These analyses showed that the content of galactose
476 and glucose was decreased, whereas the content of xylose and lignin was increased in the
477 transgenic lines compared to WT (Table 1). Thus, the analysis confirmed the increased

478 lignin to cellulose ratio in the transgenic lines seen by FT-IR and additionally revealed
479 increased xylan and reduced galactan content. Low xylan and high galactan contents are
480 diagnostic for gelatinous fibres found in tension wood in aspen (Mellerowicz &
481 Gorshkova, 2012), and therefore the observed changes in cell wall monosaccharide
482 composition suggest a decreased tension wood content in the stems of transgenic lines as
483 compared to WT.

484 ***Effects of altered PtxtXyn10A expression on cell wall architecture***

485 Based on the results for *PtxtXyn10A* expression (Figs S4; Aspeborg *et al.*, 2005;
486 Andersson-Gunnerås *et al.*, 2006; Winzell *et al.*, 2010), we anticipated its involvement
487 during secondary cell wall formation. Therefore, wood cross sections were analysed in
488 transgenic and WT plants by light and transmission electron microscopy (Fig. S5).
489 However, no major changes were detected. Light microscopy of isolated wood cells
490 revealed a small reduction in fibre diameter and length and a corresponding small
491 increase in wood density (Fig. S6). We also noted a significant change in the slit pit
492 angles in the fibres (Fig. 8a). Since the slit pit orientation corresponds to the cellulose
493 microfibril orientation in the S2 layer (Donaldson, 2008), we tested whether the reduced
494 **endo**transglycosylase activity affected the cellulose microfibril angle (MFA) in the
495 transgenic lines by performing X-ray diffraction analysis of the transgenic and WT wood
496 samples. To remove the potential effects of variable tension wood content in these
497 samples, the cellulose crystallite width was used to identify samples containing tension
498 wood. Whereas the majority of WT and transgenic antisense samples had an average
499 crystallite width between 29 and 31 Å, within the range typically reported for *Populus*
500 wood (Yamamoto *et al.*, 2010; Leppänen *et al.*, 2011), approximately one third of the
501 samples exhibited crystallite widths greater than 31 Å, typical for tension wood
502 (reviewed by Mellerowicz & Gorshkova, 2012). These samples were set aside as tension
503 wood enriched samples. Cellulose MFA in the remaining normal wood samples was
504 clearly reduced in the transgenic antisense lines (Fig. 8b), indicating that Xyn10A activity
505 is needed to orient cellulose microfibrils at large angles to the fibre axis in secondary
506 walls.

507 To investigate if the morphology of cellulose microfibrils was also affected, the topology

508 of cell walls was visualized by field emission scanning electron microscopy (FE-SEM).
 509 The images revealed an ordered, strictly parallel, dense array of microfibrils in the S2
 510 layer in all genotypes (Fig. 8c). The microfibrils had a “Z” orientation, similar to the
 511 pattern previously reported for conifers (Abe *et al.*, 1992). No major change in
 512 microfibril topology was observed in the transgenic antisense line, except for a more
 513 axial microfibril orientation as compared to WT.

514 ***Analysis of global gene expression pattern in transgenic antisense plants***

515 To investigate the effects of reduced *PtxtXyn10A* expression on the transcriptome, the
 516 global transcript profiles of developing xylem stem tissues of lines 2, 32 and WT were
 517 analysed using a 25K *Populus* (POP2) microarray (Sterky *et al.*, 2004). 123 genes were
 518 affected ($P \leq 0.05$ and $B \geq 0$) in both antisense lines, of which 76 were downregulated
 519 (Tables S3 and S4). More genes were significantly affected in line 2 than 32, in
 520 agreement with the stronger *PtxtXyn10A* suppression in this line. 61 of the affected genes
 521 could be assigned functional categories, which included signal transduction, carbohydrate
 522 metabolism and cell wall, transcription and translation, energy, cell division and cellular
 523 transport. Among the signal transduction related transcripts, several stress perception and
 524 ethylene-signalling transcripts were affected, including ones possibly involved in
 525 mechano-perception (leucine-rich receptor-like kinases, Ca-signalling related proteins,
 526 microtubule-associated proteins), which were upregulated (Table 2). Within the cell wall
 527 related category, the most striking change was the downregulation of cellulose
 528 biosynthesis related genes, including *COBRA-LIKE 4*, *FRUCTOKINASE* and *CEL9A1*
 529 (*Populus* ortholog of *KORRIGANI*), and fasciclin-like arabinogalactan proteins, which
 530 are the markers of tension wood formation (Lafarguette *et al.*, 2004; Andersson-Gunnerås
 531 *et al.*, 2006). In contrast, the expression of *PHENYLALANINE AMMONIA-LYASE*
 532 (*PAL1*) responsible for the first step of the lignin biosynthetic pathway was increased
 533 (Table 2). Over 60% of the genes downregulated in transgenic antisense lines (Table S2)
 534 were upregulated during the tension wood response (Andersson-Gunnerås *et al.*, 2006),
 535 strongly indicating that downregulation of *PtxtXyn10A* affects the tension wood and
 536 stress responses and that tension wood formation was inhibited in the transgenic antisense
 537 lines.

538 Discussion

539 *PtxtXyn10A encodes a xylan endotransglycosylase*

540 GH10 xylanases follow a retaining catalytic mechanism similar to that of xyloglucan
541 endotransglucosylases (Henrissat *et al.*, 2001), which allows both xylanase and xylan
542 endotransglycosylase activities. In plants, xylanase activity of GH10 enzymes was
543 demonstrated in cereals during caryopsis germination and pollen development (Bih *et al.*,
544 1999; Caspers *et al.*, 2001; Wu *et al.*, 2002). Recently, several vascular plants were
545 shown to have extractable xylanase and xylan endotransglycosylase activities, the latter
546 activity increasing at high 1,4- β -xylo-oligosaccharide concentration (Franková & Fry,
547 2011; Johnston *et al.*, 2013). Here, we have shown that these activities are also present in
548 developing wood of aspen (Fig. 2). Four lines of evidence indicate that *PtxtXyn10A* is
549 responsible for the observed xylan endotransglycosylase activity in developing wood.
550 First, *PtxtXyn10A* is the main GH10 enzyme expressed in this tissue (Fig. S 4). Second,
551 the heterologous expression of *PtxtXyn10A* in *Arabidopsis* protoplasts increased xylan
552 endotransglycosylase, whereas xylanase activity was not affected (Fig. 3). Third, the
553 downregulation of *PtxtXyn10A* in hybrid aspen suppressed xylan endotransglycosylase
554 activity without affecting xylanase activity (Fig. 4). Fourth, the suppression of
555 *PtxtXyn10A* activity in hybrid aspen did not result in an increased glucuronoxylan
556 molecular weight as would be expected if it were an endoxylanase (Table S2).

557 *PtxtXyn10A undergoes proteolytic processing and is transported to the apoplasm via a* 558 *non-classical pathway*

559 The size of the *PtxtXyn10A* protein detected in the cell wall bound protein fraction
560 provides clues to its processing, which according to the predicted cleavage site would
561 leave CBM22_3 and the catalytic domain in the mature protein (Fig. 1). The role of the
562 processing is presently unclear, but it does not seem to be a limiting step in the protein
563 biosynthesis as we never observed the full-length peptide even after overexpressing the
564 full length cDNA (data not shown), indicating that the processing step must be very
565 rapid. Several plant xylanases have been reported to undergo proteolytic processing, and
566 in those cases, a single CBM22 and sometimes an additional short peptide at the C-

567 terminal end are removed (Caspers *et al.*, 2001; Wu *et al.*, 2002; Chen & Paull, 2003;
568 Van Campenhout *et al.*, 2007; De Backer *et al.*, 2010). Processing has been suggested to
569 increase xylanase activity and facilitate secretion to the apoplasm (Caspers *et al.*, 2001;
570 De Backer *et al.*, 2010), but the responsible protease and mechanism of transport
571 facilitation are still unknown.

572 All known plant GH10 enzymes are active in the cell wall and mechanisms of their
573 transport to this compartment vary. Aleurone layer and tapetum xylanases accumulate in
574 cytoplasm and are released to endosperm or developing pollen grains, respectively,
575 following programmed cell death and disintegration of their source cells (Bih *et al.*, 1999;
576 Caspers *et al.*, 2001). In contrast, papaya *CpaEXY1* is secreted via the classical ER-Golgi
577 route with participation of the signal peptide (Chen & Paull, 2003). Although both
578 *PtxtXyn10A* and its orthologue *AtXyn1* lack the predicted signal peptide, they
579 accumulate in the cell wall (Fig. 1; Suzuki *et al.*, 2002) after being transported via a non-
580 classical pathway (Agrawal *et al.*, 2010).

581 ***Suppression of PtxtXyn10 activity stimulates primary growth***

582 The stimulatory effects of *PtxtXyn10A* suppression on stem elongation, leaf expansion
583 and the number of internodes observed in this study are intriguing (Fig. 5). The lack of
584 accompanying cell size increase as found for leaf epidermis and xylem cells strongly
585 indicates that these effects are not mediated by primary wall plasticity but rather related
586 to metabolism of xylan in secondary walls. The observed growth stimulation could be
587 mediated by mechanical or oligosaccharide signalling. It is also possible that the
588 suppression of xylan **endo**transglycosylase activity in spirally thickened protoxylem
589 elements changes their mechanical properties, such that they are more easily stretched
590 during organ growth, which in turn most likely leads to increased primary organ
591 expansion (Paolillo & Rubin, 1991).

592 ***PtxtXyn10 activity regulates MFA in secondary walls, probably by affecting mechano-*** 593 ***perception***

594 *PtxtXyn10A* is co-regulated with xylan biosynthesis genes during secondary wall
595 formation (Mellerowicz & Sundberg, 2008) and induced by *PtMYB021*, the transcription

596 factor responsible for secondary wall initiation (Winzéll *et al.*, 2010). It is also strongly
597 downregulated during tension wood formation (Andersson-Gunnerås *et al.*, 2006). These
598 expression patterns indicate that the encoded xylan **endo**transglycosylase plays a specific
599 role during secondary wall biosynthesis.

600 Our results show that although *PtxtXyn10A* activity neither affects xylan chain length
601 (Table S2) nor its branching pattern (Fig. 6), its suppression affects many aspects of plant
602 development, *i.e.* cellulose orientation in secondary walls (Fig. 8), tension wood
603 formation (Tables 1 & 2) and plant primary growth (Fig. 5). We propose that analogous
604 to xyloglucan endotransglucosylase activity, which releases tension in primary cell wall
605 during growth, xylan **endo**transglycosylase activity may release tension in secondary
606 walls. Such tension is envisaged to arise during self-assembly of the cellulose-xylan
607 network, during which cellulose microfibrils are deposited along rigid cortical
608 microtubules that orient the cellulose network (Baskin, 2001; Gardiner *et al.*, 2003;
609 Funada, 2008; Li *et al.*, 2012) and are immediately coated by negatively charged
610 glucuronoxytan (Stevanic & Salmén, 2009). It has been suggested that the
611 glucuronoxytan coat on the surface of cellulose microfibrils creates repulsive electrostatic
612 forces (Reis & Vian, 2004). The fact that such repulsive forces operate in cell wall can be
613 deduced from the behaviour of negatively charged cellulose crystals in solution; at high
614 concentrations, the cellulose fibrils arrange spontaneously in regular patterns forming
615 liquid crystals (Reis *et al.*, 1991; Lagerwall *et al.*, 2014). Another source of tension
616 stresses is the cross linking of microfibrils by xylan.

617 If the role of *PtxtXyn10A* is to relieve such growth stresses, its suppression would result
618 in excessive build-up of stresses that would trigger mechano-perception reactions.
619 Although very little is known about mechano-perception in plants, the emerging picture
620 points towards cortical microtubules as effectors of tensional stress signals (Jacques *et*
621 *al.*, 2013; Landrein & Hamant, 2013). Cortical microtubules assume either a random or
622 parallel orientation under control of Katanin and SPIRAL2 (Wightman *et al.*, 2013), and
623 can reorient within hours following different stimuli (Lindeboom *et al.*, 2013), resulting
624 in a change in MFA. Thus, we suggest that *PtxtXyn10A* suppression may trigger
625 mechano-perception, which in turn re-orient cortical microtubules, resulting in the
626 reduction of MFA (Fig. 9).

627 Since tension wood induction is thought to involve mechano-perception, another
628 prediction that follows from our hypothesis is that the suppression of xylan
629 **endo**transglycosylase activity may interfere with the tension wood response. The
630 observed effects in aspen (Tables 1 & 2) are compatible with this hypothesis.

631 Other factors affecting cell wall self-assembly, for example pectin metabolism (Yoneda
632 *et al.*, 2010) or fasciclin-domain arabinogalactan proteins FLA11 and FLA12 (MacMillan
633 *et al.*, 2010), are believed to influence the orientation of cellulose microfibrils. Several
634 authors have suggested that glucuronoxylan plays a role in determining MFA (Reis &
635 Vian, 2004; Ruel *et al.*, 2006). Its abundance and MFA in different secondary wall layers
636 were shown to be correlated in radiata pine (Donaldson & Knox, 2012). Moreover, in
637 white spruce, the *Xyn10* locus was found to be associated with MFA (Beaulieu *et al.*,
638 2011). Here, we have provided empirical evidence that *PtxtXyn10A* affects MFA in wood
639 fibres in hybrid aspen and proposed a mechanism for such regulation.

640

641 **Acknowledgements**

642 We thank Kjell Olofsson, Andreas Sjödin and Oskar Skogström, Laszlo Bako, Kirsi
643 Leppänen and Gaia Geiss for help with the anatomy, microarrays, protoplasts, X-ray and
644 qPCR analyses, respectively, and Anne Gouget, Lorenz Gerber and Tarek Elhasi for
645 preliminary experiments. András Gorzsás from the Vibrational Spectroscopy Platform at
646 Umeå University assisted with the FTIR spectroscopic analysis **and Cheng Choo Lee at**
647 **the Umeå Electron Microscopy Core Facility with FE-SEM.**

648

649 **Literature Cited**

650 **Abe H, Ohtani J, Fukazawa K. 1992.** Microfibrillar orientation of the innermost surface
651 of conifer tracheid wall. *IAWA Bulletin* **13**: 411–417.

652 **Agrawal GK, Jwa NS, Lebrun MH, Job D, Rakwal R. 2010.** Plant secretome:
653 Unlocking secrets of the secreted proteins. *Proteomics* **10**: 799–827.

654 **Akin E, Himmelsbach DS, Carl RT, Hanna WW, Barton FE II. 1993.** Mid-infrared

- 655 microspectroscopy to assess lignin in plant tissues related to digestibility. *Agronomy*
656 *Journal* **85**: 171–175.
- 657 **Andersson-Gunnerås S, Mellerowicz EJ, Love J, Segerman B, Ohmiya Y, Coutinho**
658 **PM, Nilsson P, Henrissat B, Moritz T, Sundberg B. 2006.** Biosynthesis of cellulose-
659 enriched tension wood in *Populus*: global analysis of transcription and metabolites
660 identifies biochemical and developmental regulators in secondary wall biosynthesis.
661 *Plant Journal* **45**: 144–165.
- 662 **Aspeborg H, Schrader J, Coutinho PM, Stam M, Kallas Å, Djerbi S, Nilsson P,**
663 **Denman S, Amini B, Sterky F et al. 2005.** Carbohydrate-active enzymes involved in the
664 secondary cell wall biogenesis in hybrid aspen. *Plant Physiology* **137**: 983–997.
- 665 **Awano T, Takabe K, Fujita M. 2002.** Xylan deposition on secondary wall of *Fagus*
666 *crenata* fiber. *Protoplasma* **219**: 106–115.
- 667 **Banik M, Garrett TPJ, Fincher GB. 1996.** Molecular cloning of cDNAs encoding (14)-
668 β -xylan endohydrolases from the aleurone layer of germinated barley (*Hordeum*
669 *vulgare*). *Plant Molecular Biology* **31**: 1163–1172.
- 670 **Baskin TI. 2001.** On the alignment of cellulose microfibrils by cortical microtubules: a
671 review and a model. *Protoplasma* **215**: 150–171.
- 672 **Beaulieu J, Doerksen T, Boyle B, Clément S, Deslauriers M, Beauseigle S, Blais S,**
673 **Poulin PL, Lenz P, Caron S et al. 2011.** Association genetics of wood physical traits in
674 the conifer white spruce and relationships with gene expression. *Genetics* **188**: 197–214.
- 675 **Benjavongkulchai E, Spencer MS. 1986.** Purification and characterization of barley-
676 aleurone xylanase. *Planta* **169**: 415–419.
- 677 **Bevan MW, Franssen MCR. 2006.** Investing in green and white biotech. *Nature*
678 *Biotechnology* **24**: 765–767.
- 679 **Bih FY, Wu SS, Ratnayake C, Walling LL, Nothnagel EA, Huang AH. 1999.** The
680 predominant protein on the surface of maize pollen is an endoxylanase synthesized by a
681 tapetum mRNA with a long 5' leader. *Journal of Biological Chemistry* **274**: 22884–
682 22894.

- 683 **Biswal AK, Soeno K, Latha Gandla M, Immerzeel P, Pattathil S, Lucenius J,**
684 **Serimaa R, Hahn MG, Moritz T, Jönsson LJ, Israelsson-Nordström M, Mellerowicz**
685 **EJ. 2014.** Aspen pectate lyase *PtxtPL1-27* mobilizes matrix polysaccharides from
686 woody tissues and improves saccharification yield. *Biotechnology for Biofuels* 7:11.
- 687 **Busse-Wicher M, Gomes TCF, Tryfona T, Nikolovski N, Stott K, Grantham NJ,**
688 **Bolam DN, Skaf MS, Dupree P. 2014.** The pattern of xylan acetylation suggests xylan
689 may interact with cellulose microfibrils as a two-fold helical screw in the secondary plant
690 cell wall of *Arabidopsis thaliana*. *Plant Journal* in press.
- 691 **Bromley JR, Busse-Wicher M, Tryfona T, Mortimer JV, Zhang Z, Brown D,**
692 **Dupree P. 2013.** GUX1 and GUX2 glucuronyltransferases decorate distinct domains of
693 glucuronoxylan with different substitution patterns. *Plant Journal* 74: 423–434.
- 694 **Brummell DA, Schröder R. 2009.** Xylan metabolism in primary cell walls. *New*
695 *Zealand Journal of Forestry Science* 39: 125–143.
- 696 **Caspers MPM, Lok F, Sinjorgo KMC, van Zeijl MJ, Nielsen KA, Cameron-Mills V.**
697 **2001.** Synthesis, processing and export of cytoplasmic *endo*-beta-1,4-xylanase from
698 barley aleurone during germination. *Plant Journal* 26:191–204.
- 699 **Charnock SJ, Lakey JH, Virden R, Hughes N, Sinnott ML, Hazelwood GP,**
700 **Pickergill R, Gilbert HJ. 1997.** Key residues in subsite f play a critical role in the
701 activity of *Pseudomonas fluorescens* subspecies *cellulosa* xylanase against
702 xylooligosaccharides but not against highly polymeric substrates such as xylan. *Journal*
703 *of Biological Chemistry* 272: 2942–2951.
- 704 **Chen NJ, Paull RE. 2003.** Endoxylanase expressed during papaya fruit ripening:
705 purification, cloning and characterization. *Functional Plant Biology* 30: 433–441.
- 706 **Cleemput G, Hessing M, Van Oort M, Deconynck M, Delcour JA. 1997a.** Purification
707 and characterization of a beta-D-xylosidase and an *endo*-xylanase from wheatflour. *Plant*
708 *Physiology* 113: 377–386.
- 709 **Cleemput G, Van Laere K, Hessing M, Van Leuven F, Torrekens S, Delcour JA.**
710 **1997b.** Identification and characterization of a novel arabinoxylanase from wheat flour.
711 *Plant Physiology* 115: 1619–1627.

- 712 **Clough SJ, Bent AF. 1998.** Floral dip: a simplified method for *Agrobacterium*-mediated
713 transformation of *Arabidopsis thaliana*. *Plant Journal* **16**: 735–743.
- 714 **Darvill JE, Mcneil M, Darvill AG, Albersheim P. 1980.** Structure of plant-cell walls.
715 II. Glucuronoarabinoxylan, a 2nd hemicellulose in the primary-cell walls of suspension-
716 cultured sycamore cells. *Plant Physiology* **66**: 1135–1139.
- 717 **De Backer E, Gebruers K, Van den Ende W, Courtin CM, Delcour JA. 2010.** Post-
718 translational processing of beta-d-xylanases and changes in extractability of
719 arabinoxylans during wheat germination. *Plant Physiology and Biochemistry* **48**: 90–97.
- 720 **Dóczy R, Hatzimasoura E, Bögre L. 2011.** Mitogen-activated protein kinase activity and
721 reporter gene assays in plants. *Methods in Molecular Biology* **779**: 79–92.
- 722 **Dokken KM, Davis LC, Marinkovic NS. 2005.** Use of infrared microspectroscopy in
723 plant growth and development. *Applied Spectroscopy Reviews* **40**: 301–326.
- 724 **Donaldson LA. (2008)** Microfibril angle: measurement, variation and relationships – a
725 review. *IAWA Journal* **29**: 345–386.
- 726 **Donaldson LA, Knox JP. 2012.** Localization of cell wall polysaccharides in normal and
727 compression wood of radiata pine: relationships with lignification and microfibril
728 orientation. *Plant Physiology* **158**: 642–653.
- 729 **Ebringerová A, Heinze T. 2000.** Xylan and xylan derivatives – biopolymers with
730 valuable properties. Naturally occurring xylan structures, procedures and properties.
731 *Macromolecular Rapid Communications* **21**: 542–556.
- 732 **Franková L, Fry SC. 2011.** Phylogenetic variation in glycosidases and glycanases acting
733 on plant cell wall polysaccharides, and the detection of transglycosidase and trans- β -
734 xylanase activities. *Plant Journal* **67**: 662–681.
- 735 **Franková L, Fry SC. 2013.** Biochemistry and physiological roles of enzymes that ‘cut
736 and paste’ plant cell-wall polysaccharides. *Journal of Experimental Botany* **64**: 3519–
737 3550.
- 738 **Fry S. 2004.** Primary cell wall metabolism: tracking the careers of wall polymers in
739 living plant cells. *New Phytologist* **161**: 641–675.

- 740 **Funada R. 2008.** Microtubules and the control of wood formation. In: Nick P, editor.
741 *Plant microtubules: development and flexibility*. Springer-Verlag, Berlin, pp 83–119.
- 742 **Gardiner JC, Taylor NG, Turner SR. 2003.** Control of cellulose synthase complex
743 localization in developing xylem. *Plant Cell* **15**: 1740–1748.
- 744 **Geisler-Lee J, Geisler M, Coutinho PM, Segerman B, Nishikubo N, Takahashi J,**
745 **Aspeborg H, Djerbi S, Master E, Andersson-Gunnerås S et al. 2006.** Poplar
746 carbohydrate-active enzymes. Gene identification and expression analyses. *Plant*
747 *Physiology* **140**: 946–962.
- 748 **Goubet F, Jackson P, Deery MJ, Dupree P. 2002.** Polysaccharide analysis using
749 carbohydrate gel electrophoresis. A method to study plant cell wall polysaccharides and
750 polysaccharide hydrolases. *Analytical Biochemistry* **300**: 53–68.
- 751 **Goujon T, Minic Z, El Amrani A, Lerouxel O, Aletti E, Lapierre C, Joseleau JP,**
752 **Jouanin L. 2003.** *AtBXL1*, a novel higher plant (*Arabidopsis thaliana*) putative beta-
753 xylosidase gene, is involved in secondary cell wall metabolism and plant development.
754 *Plant Journal* **33**: 677–690.
- 755 **Gray-Mitsumune M, Abe H, Takahashi J, Sundberg B, Mellerowicz EJ. 2004.**
756 Liquid phase fluorescence in situ RT-PCR analysis for gene expression analysis in woody
757 stems. *Plant Biology* **6**: 47–54.
- 758 **Gray-Mitsumune M, Blomquist K, McQueen-Mason S, Teeri TT, Sundberg B,**
759 **Mellerowicz EJ. 2008.** Ectopic expression of a wood-abundant expansin *PttEXPA1*
760 promotes cell expansion in primary and secondary tissues in aspen. *Plant Biotechnology*
761 *Journal* **6**: 62–72.
- 762 **Henrissat B, Coutinho PM, Davies GJ. 2001.** A census of carbohydrate-active enzymes
763 in the genome of *Arabidopsis thaliana*. *Plant Molecular Biology* **47**: 55–72.
- 764 **Hertzberg M, Aspeborg H, Schrader J, Andersson A, Erlandsson R, Blomqvist K,**
765 **Bhalerao R, Uhlen M, Teeri TT, Lundeberg J et al. 2001.** A transcriptional road map
766 to wood formation. *Proceeding of the National Academy of Sciences of the United States*
767 *of America* **98**: 14732–14737.
- 768 **Ichinose H, Nishikubo N, Demura T, Kaneko S. 2010.** Characterization of a-L-

- 769 arabinofuranosidase related to the secondary cell walls formation in *Arabidopsis*
770 *thaliana*. *Plant Biotechnology* **27**: 259–266.
- 771 **Imamura T, Watanabe T, Kuwahara M, Koshijima T. 1994.** Ester linkages between
772 lignin and glucuronic-acid in lignin-carbohydrate complexes from *Fagus crenata*.
773 *Phytochemistry* **37**: 1165–1173.
- 774 **Jacobs A, Dahlman O. 2001.** Characterization of the molar masses of hemicelluloses
775 from wood and pulps employing size exclusion chromatography and matrix-assisted laser
776 desorption ionization time-of-flight mass spectrometry. *Biomacromolecules* **2**: 894–905.
- 777 **Jacques E, Verbelen J-P, Vissenberg K. 2013.** Mechanical stress in *Arabidopsis* leaves
778 orients microtubules in a ‘continuous’ supracellular pattern. *BMC Plant Biology* **13**:163.
- 779 **Johnston SL, Prakash R, Chen NJ, Kumagai MH, Turano HM, Cooney JM,**
780 **Atkinson RG, Paull RE, Cheetamun R, Bacic A et al. 2013.** An enzyme activity
781 capable of endotransglycosylation of heteroxylan polysaccharides is present in plant
782 primary cell walls. *Planta* **237**: 173–187.
- 783 **Kabel MA, van den Borne H, Vincken JP, Voragen Schols HA. 2007.** Structural
784 differences of xylans affect their interaction with cellulose. *Carbohydrate Polymers* **69**:
785 94–105.
- 786 **Karimi M, Inzé D, Depicker A. 2002.** Gateway vectors for *Agrobacterium*-mediated
787 plant transformation. *Trends in Plant Science* **7**: 193–195.
- 788 **Kosík O, Garajová S, Matulová M, Rehulka P, Stratilová E, Farkaš V. 2011.** Effect
789 of the label of oligosaccharide acceptors on the kinetic parameters of nasturtium seed
790 xyloglucan endotransglycosylase (XET). *Carbohydrate Research* **346**: 357–361.
- 791 **Kosik O, Bromley JR, Busse-Wicher M, Zhang Z, Duprée P. 2012.** Studies of
792 enzymatic cleavage of cellulose using polysaccharide analysis by carbohydrate gel
793 electrophoresis (PACE). *Methods in Enzymology* **510**: 51–67.
- 794 **Lafarguette F, Leple JC, Dejardin A, Laurans F, Costa G, Lesage-Descauses MC,**
795 **Pilate G. 2004.** Poplar genes encoding fasciclin-like arabinogalactan proteins are highly
796 expressed in tension wood. *New Phytologist* **164**: 107–121.

- 797 **Lagerwall JPF, Schütz C, Salajkova M, Noh JH, Park JH, Scalia G, Bergström L.**
798 **2014.** Cellulose nanocrystal-based materials: from liquid crystal self-assembly and glass
799 formation to multifunctional thin films. *NPG Asia Materials* **6**: e80
- 800 **Landrein B, Hamant O. 2013.** How mechanical stress controls microtubule behavior
801 and morphogenesis in plants: history, experiments and revisited theories. *Plant Journal*
802 **75**: 324–338.
- 803 **Larsson M, Gräslund S, Yuan L, Brundell E, Uhlén M, Höög C, Ståhl S. 2000.** High-
804 throughput protein expression of cDNA products as a tool in functional genomics.
805 *Journal of Biotechnology* **80**: 143–157.
- 806 **Latha Gandla M, Derba-Maceluch M, Liu X, Gerber L, Master ER, Mellerowicz**
807 **EJ, Jönsson LJ. 2014.** Expression of a fungal glucuronoyl esterase in *Populus*: effects
808 on wood properties and saccharification efficiency. *Phytochemistry*, in press.
- 809 **Lee C, Teng Q, Huang W, Zhong R, Ye ZH. 2011.** Molecular dissection of xylan
810 biosynthesis during wood formation in poplar. *Molecular Plant* **4**: 730–747.
- 811 **Leppänen K, Bjurhager I, Peura M, Kallonen A, Suuronen JP, Penttilä P, Love J,**
812 **Fagerstedt K, Serimaa R. 2011.** X-ray scattering and microtomography study on the
813 structural changes of never-dried silver birch, European aspen and hybrid aspen during
814 drying. *Holzforschung* **65**: 865–873.
- 815 **Lever M. 1972.** A new reaction for colorimetric determination of carbohydrates.
816 *Analytical Biochemistry* **47**: 273–279.
- 817 **Li S, Lei L, Somerville C, Gu Y. 2012.** Cellulose synthase interactive protein1 (CS11)
818 links microtubules and cellulose synthase complexes. *Proceeding of the National*
819 *Academy of Sciences of the United States of America* **109**: 185–190.
- 820 **Li XL, SpánikováS, de Vries RP, Biely P. 2007.** Identification of genes encoding
821 microbial glucuronoyl esterases. *FEBS Letters* **581**: 4029–4035.
- 822 **Lindeboom JJ, Nakamura M, Hibbel A, Shundyak K, Gutierrez R, Ketelaar T,**
823 **Emons AMC, Mulder BM, Kirik V, Ehrhardt DW. 2013.** A mechanism for
824 reorientation of cortical microtubule arrays driven by microtubule severing. *Science* **342**:
825 1245533.

- 826 **Livak KJ, Schmittgen TD. 2001.** Analysis of relative gene expression data using real-
827 time quantitative PCR and the $2^{(-\Delta\Delta C(T))}$ method. *Methods* **25**: 402–408.
- 828 **MacMillan CP, Mansfield SD, Stachurski ZH, Evans R, Southerton SG. 2010.**
829 Fasciclin-like arabinogalactan proteins: specialization for stem biomechanics and cell
830 wall architecture in *Arabidopsis* and *Eucalyptus*. *Plant Journal* **62**: 689–703.
- 831 **McCartney L, Blake AW, Flint J, Bolam DN, Boraston AB, Gilbert HJ, Knox JP.**
832 **2006.** Differential recognition of plant cell walls by microbial xylan-specific
833 carbohydrate-binding modules. *Proceeding of the National Academy of Sciences of the*
834 *United States of America* **103**: 4765–4770.
- 835 **Mellerowicz EJ, Baucher M, Sundberg B, Boerjan W. 2001.** Unravelling cell wall
836 formation in the woody dicot stem. *Plant Molecular Biology* **47**: 239–274.
- 837 **Mellerowicz EJ, Sundberg B. 2008.** Wood cell walls: biosynthesis, developmental
838 dynamics and their implications for wood properties. *Current Opinion in Plant Biology*
839 **11**: 293–300.
- 840 **Mellerowicz EJ, Gorshkova T. 2012.** Tensional stress generation in gelatinous fibres: a
841 review and possible mechanism based on cell wall structure and composition. *Journal of*
842 *Experimental Botany* **63**: 551–565.
- 843 **Minic Z, Jouanin L. 2006.** Plant glycoside hydrolases involved in cell wall
844 polysaccharide degradation. *Plant Physiology and Biochemistry* **44**: 435–449.
- 845 **Naran R, Black S, Decker SR, Azadi P. 2009.** Extraction and characterization of native
846 heteroxylans from delignified corn stover and aspen. *Cellulose* **16**: 661–675.
- 847 **Paolillo Jr DJ, Rubin G. 1991.** Relative elemental rates of elongation and the
848 protoxylem-metaxylem transition in hypocotyls of soybean seedlings. *American Journal*
849 *of Botany* **78**: 845–854.
- 850 **Paul RE, Chen NJ. 1983.** Postharvest variation in cell wall-degrading enzymes of
851 papaya (*Carica papaya* L.) during fruit ripening. *Plant Physiology* **72**: 382–385.

- 852 **Reis D, Vian B, Chanzy H, Roland JC. 1991.** Liquid crystal-type assembly of native
853 cellulose-glucuronoxylans extracted from plant cell wall. *Biology of the Cell* **73**: 173–
854 178.
- 855 **Reis D, Vian B. 2004.** Helicoidal pattern in secondary cell walls and possible role of
856 xylans in their construction. *Comptes Rendus Biologies* **327**: 785–790.
- 857 **Rennie EA, Scheller HV. 2014.** Xylan biosynthesis. *Current Opinion in Biotechnology*
858 **26**:100–107.
- 859 **Rogowski A, Baslé A, Farinas CS, Solovyova A, Mortimer JC, Dupree P, Gilbert**
860 **HJ, Bolam DN. 2014.** Evidence that GH115 α -glucuronidase activity, which is required
861 to degrade plant biomass, is dependent on conformational flexibility. *The Journal of*
862 *Biological Chemistry*: **289**: 53–64.
- 863 **Ruel K, Chevalier-Billosta V, Guillemin F, Sierra JB, Joseleau JP. 2006.** The wood
864 cell wall at the ultrastructural scale – formation and topochemical organization Maderas.
865 *Ciencia y tecnología* **8**: 107–116.
- 866 **Scheller HV, Ulvskov P. 2010.** Hemicelluloses. *Annual Review of Plant Biology* **61**:
867 263–289.
- 868 **Simpson DJ, Fincher GB, Huang AHC, Cameron-Mills V. 2003.** Structure and
869 function of cereal and related higher plant (1 \rightarrow 4)-beta-xylan endohydrolases. *Journal of*
870 *Cereal Science* **37**: 111–127.
- 871 **Sjödín A, Bylesjö M, Skogström O, Eriksson D, Nilsson P, Rydén P, Jansson S,**
872 **Karlsson J. 2006.** UPSC-BASE - *Populus* transcriptomics online. *Plant Journal* **48**:
873 806–817.
- 874 **Slade AM, Hoj PB, Morrice NA, Fincher GB. 1989.** Purification and characterization
875 of three (1 \rightarrow 4)- β -D-xylan endohydrolases from germinated barley. *European Journal of*
876 *Biochemistry* **185**: 533–539.
- 877 **Spániková S, Biely P. 2006.** Glucuronoyl esterase – novel carbohydrate esterase
878 produced by *Schizophyllum commune*. *FEBS Letters* **580**: 4597–4601.
- 879 **Spániková S, Polakova M, Joniak D, Hirsch J, Biely P. 2007.** Synthetic esters

- 880 recognized by glucuronoyl esterase from *Schizophyllum commune*. *Archives of*
881 *Microbiology* **188**: 185–189.
- 882 **Sterky F, Bhalerao RR, Unneberg P, Segerman B, Nilsson P, Brunner AM, Campaa**
883 **L, Jonsson LJ, Tandre K, Strauss SH et al. 2004.** A *Populus* EST resource for plant
884 functional genomics. *Proceeding of the National Academy of Sciences of the United*
885 *States of America* **101**: 13951–13956.
- 886 **Stevanic JS, Salmén. 2009.** Orientation of the wood polymers in the cell wall of spruce
887 wood fibres. *Holzforschung* **63**: 497–503.
- 888 **Stewart D, Yahiaoui N, McDougall GJ, Myton K, Marque C, Boudet AM, Haigh J.**
889 **1997.** Fourier-transform infrared and Raman spectroscopic evidence for the incorporation
890 of cinnamaldehydes into the lignin of transgenic tobacco (*Nicotiana tabacum* L.) plants
891 with reduced expression of cinnamyl alcohol dehydrogenase. *Planta* **201**: 311–318.
- 892 **Svedström K, Lucenius J, Van den Bulcke J, Van Loo D, Immerzeel P, Suuronen J-**
893 **P, Brabant L, Van Acker J, Saranpää P, Fagerstedt K et al. 2012.** Hierarchical
894 structure of juvenile hybrid aspen xylem revealed using x-ray scattering and
895 microtomography. *Trees-Structure and Function* **26**: 1793–1804.
- 896 **Suen DF, Huang AHC. 2006.** Maize pollen coat xylanase facilitates pollen tube
897 penetration into silk during sexual reproduction. *Journal of Biological Chemistry* **282**:
898 625–636.
- 899 **Suzuki M, Kato A, Nagata N, Komeda Y. 2002.** A Xylanase, AtXyn1, is predominantly
900 expressed in vascular bundles, and four putative xylanase genes were identified in the
901 *Arabidopsis thaliana* genome. *Plant and Cell Physiology* **43**: 759–767.
- 902 **Takahashi J, Rudsander UJ, Hedenström M, Banasiak A, Harholt J, Amelot N,**
903 **Immerzeel P, Ryden P, Endo S, Ibatullin FM et al. 2009.** *KORRIGAN1* and its aspen
904 homolog *PttCel9A1* decrease cellulose crystallinity in *Arabidopsis* stems. *Plant and Cell*
905 *Physiology* **50**: 1099–1115.
- 906 **Teleman A, Lundqvist J, Tjerneld F, Stålbrand H, Dahlman O. 2000.**
907 Characterization of acetylated 4-*O*-methylglucuronoxylan isolated from aspen employing
908 ¹H and ¹³C NMR spectroscopy. *Carbohydrate Research* **329**: 807–815.

- 909 **Theander O, Westerlund EA. 1986.** Studies on dietary fiber. 3. Improved procedures
910 for analysis of dietary fiber. *Journal of Agricultural and Food Chemistry* **34**: 330–336.
- 911 **Timell TE. 1967.** Recent progress in the chemistry of wood hemicellulose. *Wood Science*
912 *and Technology* **1**: 45–70.
- 913 **Trygg J, Wold S. 2002.** Orthogonal projections to latent structures (O-PLS). *Journal of*
914 *Chemometrics* **16**: 119–128.
- 915 **Van Campenhout S, Pollet A, Bourgois TM, Rombouts S, Beaugrand J, Gebruers**
916 **K, De Backer E, Courtin CM, Delcour JA, Volckaert G. 2007.** Unprocessed barley
917 aleurone endo- β -1,4-xylanase X-I is an active enzyme. *Biochemical and Biophysical*
918 *Research Communications* **356**: 799–804.
- 919 **Vandesompele J, De Preter K, Pattyn F, Poppe B, Van Roy N, De Paepe A,**
920 **Speleman F. 2002.** Accurate normalization of real-time quantitative RT-PCR data by
921 geometric averaging of multiple internal control genes. *Genome Biology* **3**: research 34,
922 PMID:12184808.
- 923 **Wightman R, Chomicki G, Kumar M, Carr P, Turner SR. 2013.** SPIRAL2
924 determines plant microtubule organization by modulating microtubule severing. *Current*
925 *Biology* **23**: 1902–1907.
- 926 **Wilkins O, Nahal H, Foong J, Provart NJ, Campbell MM. 2009.** Expansion and
927 diversification of the *Populus* R2R3-MYB family of transcription factors. *Plant*
928 *Physiology* **149**: 981–993.
- 929 **Winz ell A, Aspeborg H, Wang Y, Ezcurra I. 2010.** Conserved CA-rich motifs in gene
930 promoters of PtxtMYB021-responsive secondary cell wall carbohydrate-active enzymes
931 in *Populus*. *Biochemical and Biophysical Research Communications* **394**: 848–853.
- 932 **Wu SSH, Suen DF, Chang HC, Huang AHC. 2002.** Maize tapetum xylanase is
933 synthesized as a precursor, processed and activated by a serine protease, and deposited on
934 the pollen. *Journal of Biological Chemistry* **277**: 49055–49064.
- 935 **Yamamoto H, Ruelle J, Arakawa Y, Yoshida M, Clair B, Gril J. 2010.** Origin of the
936 characteristic hygro-mechanical properties of the gelatinous layer in tension wood from
937 Kunugi oak (*Quercus acutissima*). *Wood Science and Technology* **44**: 149–163.

938 **Yoneda A, Ito T, Higaki T, Kutsuna N, Saito T, Ishimizu T, Osada H, Hasezawa S,**
939 **Matsui M, Demura T. 2010.** Cobtorin target analysis reveals that pectin functions in the
940 deposition of cellulose microfibrils in parallel with cortical microtubules. *Plant Journal*
941 **64:** 657–667.

942 **Zhong R, Morrison III WH, Himmelsbach DS, Poole II FL, Ye ZH. 2000.** Essential
943 role of caffeoyl coenzyme A *O*-methyltransferase in lignin biosynthesis in woody poplar
944 plants. *Plant Physiology* **124:** 563–577.

945

For Peer Review

946 **Supporting Information:**

947 **Fig. S1.** Clarification of Phytozome gene models for *PtXyn10A* and *PtXyn10H*.

948 **Fig. S2.** Phylogenetic analysis of the GH10 family in *Populus trichocarpa* and
949 *Arabidopsis thaliana*.

950 **Fig. S3.** *PtxtXyn10A* expression analyses.

951 **Fig. S4.** *Populus* GH10 family gene expression analysis.

952 **Fig. S5.** Effects of *PtxtXyn10A* expression on wood anatomy and ultrastructure.

953 **Fig. S6.** Relationship between wood cell dimensions, volumetric mass and expression
954 level of *PtxtXyn10A*.

955

956 **Supplemental Tables:**

957 **Table S1.** GH10 gene models of *P. trichocarpa*, v 7.0 (<http://www.phytozome.net/>).

958 **Table S2.** Size-exclusion chromatography parameters of hemicellulose distributions in
959 the transgenic antisense lines and WT.

960 **Table S3.** List of genes significantly ($P \leq 0.05$ and $B \geq 0$) downregulated in both
961 transgenic antisense lines 2 and 32.

962 **Table S4.** List of genes significantly ($P \leq 0.05$ and $B \geq 0$) upregulated in both transgenic
963 antisense lines 2 and 32.

964 **Table S5.** List of primers used for RT-qPCR analysis.

965 **Table S6.** List of primers used for cloning.

966 **Fig. captions**967 **Fig. 1.** *PtxtXyn10A* protein accumulates in cell walls.968 (a) Modular structure of *PtxtGT10A* showing three carbohydrate-binding modules 22
969 (CBM22) and a catalytic domain (*Xyn10*). Predicted *N*-glycosylation sites are marked,
970 along with the predicted processing site shown by an arrow.971 (b) Western blotting of soluble and cell wall bound protein fractions extracted from
972 developing xylem and apical bud tissues and probed with the antibody Kamisa raised
973 against the C-terminal fragment of *PtxtXyn10A*. A 68 kDa peptide (arrow) was detected
974 in the cell wall bound protein fraction from developing xylem.975 (c) Immunolocalisation of *PtxtXyn10A* protein fused with eGFP and stably expressed in
976 *Arabidopsis*. The root cells were plasmolyzed with 20% v/v mannitol, fixed,
977 immunolabelled against GFP protein and observed by confocal microscopy. The
978 arrowhead shows the signal from cell wall and the arrow shows the plasmolysed
979 protoplast. The negative control was assay without primary antibodies. Bar = 20 μm .980 **Fig. 2.** Xylanase and xylan **endo**transglycosylase activities are present in cell wall bound
981 protein fractions extracted from developing xylem.982 (a) Xylanase and xylan **endo**transglycosylase activities detected by thin-layer
983 chromatography of products after incubation of extracted proteins with xylohexaose
984 (Xylo_6) at either 1.25 mM or 6.25 mM concentrations, as indicated in the figure, for 1-42
985 h at 40°C. Extracts boiled for 10 min were used as negative controls. At low substrate
986 concentration, the main products had DP 1-5, indicating hydrolysis, whereas at high
987 substrate concentration, products corresponding to DP 8-10 were additionally detected,
988 indicating xylan **endo**transglycosylase activity. The DP of xylooligosaccharides was
989 determined from standards containing Xylo_1 to Xylo_6 either directly (black triangles) of
990 by interpolation (white triangles). Volumes corresponding to the same amounts of
991 substrates were loaded in each lane.992 (b) Xylan **endo**transglycosylation activity detected by ANTS assay as described in the
993 Material and Methods. The SE bars show variability among technical replicates. The
994 control reaction lacked protein extracts.

995 (c) Susceptibility of fluorescent product detected by ANTS assay for 1 h incubations with
 996 pectate lyase (PL), xylanase M1 (XylM1) or buffer (Buf; no enzymatic treatment) at
 997 40°C.

998 **Fig. 3.** Expression of *PtxtXyn10A* in *Arabidopsis* protoplasts results in strong
 999 upregulation of xylan **endo**transglycosylase but not xylanase.

1000 Protoplasts were transfected with either Xyn10A or an empty vector, and transgene
 1001 expression was verified by RT-qPCR. Mean enzymatic activity \pm SE, $n=4$ biological
 1002 replicates, P values correspond to the probability of the null hypothesis in the Fisher test.

1003 (a) Xylan **endo**transglycosylase specific activities determined by ANTS assay as
 1004 described in the Material and Methods.

1005 (b) Xylanase specific activities determined by Azo-Xylan solubilisation.

1006 (c) Xylanase specific activity determined by the formation of reducing ends.

1007 **Fig. 4.** Downregulation of *PtxtXyn10A* reduces xylan **endo**transglycosylase activity in
 1008 developing wood. **Three independent transgenic antisense lines (2, 3 and 32) are**
 1009 **compared to WT.**

1010 (a) *PtxtXyn10A* transcript levels in transgenic antisense lines and WT determined by RT-
 1011 qPCR. Data were calibrated to CYP and normalized to the WT level. Means of 3-9
 1012 biological replicates \pm SE.

1013 (b) *PtxtXyn10A* protein levels detected by the antibody Kamisa in the cell wall bound
 1014 protein extracts. The signal from an unrelated cell wall localised protein (*PtxtCel9B3*)
 1015 was used as a loading control for the transgenic antisense lines.

1016 (c) Xylan **endo**transglycosylase activity in cell wall bound protein extracts from the
 1017 transgenic antisense lines and WT. Means of 3 biological replicates \pm SE.

1018 (d) Xylanase activity in transgenic antisense lines determined by the formation of
 1019 reducing ends following incubation of the cell wall bound protein extracts with xylan.
 1020 Means of three biological replicates \pm SE. The effect of genotype was not significant
 1021 (ANOVA, $P \leq 10\%$).

1022 * indicates values significantly different from WT (t -test, 5%)

1023 **Fig. 5.** Downregulation of *PtxtXyn10A* increases plant primary growth.
 1024 Stem height, diameter, number of internodes, internode length, leaf length and width
 1025 were measured in trees after three months of growth in the greenhouse. **Average cell**
 1026 **surface area was determined for the leaf adaxial epidermis from nail polish casts.** Means
 1027 of ten biological replicates \pm SE. * indicates values significantly different from WT (*t*-
 1028 test, 5%).

1029 **Fig. 6.** Glucuronoxylan [Me]GlcA substitution pattern in transgenic antisense lines with
 1030 reduced xylan **endo**transglycosylase activity (2 and 3) and in wild-type aspen (WT).
 1031 Milled wood was hydrolysed with *BoGH30* to completion and the resulting digestion
 1032 products were analysed using polysaccharide analysis by carbohydrate gel
 1033 electrophoresis (PACE). Standards X1 to X6 (S), enzyme (E only) and wood material
 1034 only (no E) are shown. * indicates non-specific labelling product.

1035 **Fig. 7.** OPLS-DA models of diffuse reflectance Fourier-transform infrared spectra.
 1036 (a) Scores plot showing the separation of transgenic antisense plants (empty symbols;
 1037 squares: line 2, triangles: line 3, diamonds: line 32) from wild type (filled dots), using
 1038 five to six individual plants per line.
 1039 (b) Corresponding loadings plot showing factors responsible for the separation. Bands
 1040 that are referred to in the text are labelled. Bands that are positive (*i.e.* more intense in the
 1041 transgenic antisense lines) are labelled with black regular fonts, bands that are negative
 1042 (*i.e.* more intense in the wild type) are labelled with black italic fonts. The 1595 cm^{-1}
 1043 band was unchanged and is labelled with grey regular font. The model has the following
 1044 details: 1 + 1 components (predictive + orthogonal), $R^2X(\text{cum}) = 0.642$, $R^2Y(\text{cum}) =$
 1045 0.598 ; $Q^2(\text{cum}) = 0.254$.

1046 **Fig. 8.** Suppression of *PtxtXyn10A* affects orientation of cellulose microfibrils in
 1047 secondary walls of wood fibres.
 1048 (a) Orientation of slit-pits relative to fibre axis in isolated wood fibres from transgenic
 1049 antisense lines and WT visualized using Nomarski optics. Example of slit pits and their
 1050 angle is shown beside the graph.

1051 (b) Cellulose microfibril angle (MFA) measured by X-ray diffraction in samples from
1052 transgenic antisense lines and WT representing primarily normal wood after exclusion of
1053 tension wood samples based on crystallite size.

1054 For (a) and (b) Means of 3 biological replicates \pm SE. The *P* value for the difference
1055 between both transgenic antisense lines and the WT is indicated above the line.

1056 (c) Appearance of cellulose microfibrils in the transgenic antisense line 2, 3 and WT
1057 visualised by SEM. The fibres were oriented vertically and observed from the inside. The
1058 cell wall appearance was similar in the transgenic antisense lines and WT, but the
1059 microfibril angle (traced with white lines) was larger in the WT. Scale bar = 200 nm.

1060 **Fig. 9.** Proposed hypothesis of *PtxtXyn10A* action on cellulose microfibril angle.

1061 The main function of *PtxtXyn10A* is proposed to be the elimination of tension in cell
1062 wall that arises during cell wall assembly. The suppression of *PtxtXyn10A* causes the
1063 build-up of tension in the cell wall, which is sensed by mechanical sensors (tension gated
1064 Ca^{++} channels, and/or receptor leucine-rich kinases) that activate the mechanosensing
1065 signal transduction pathway, causing re-organization of cortical microtubules and
1066 subsequent re-orientation of cellulose microfibrils.

1067

1068 **Tables:**

1069 **Table 1.** Sugar composition and lignin content in the transgenic antisense lines and WT.

1070 Five trees were pooled per line, two technical replicates. Neutral sugar and lignin

1071 contents are expressed as % of the total measured yield. The yield was over 865 mg/g.

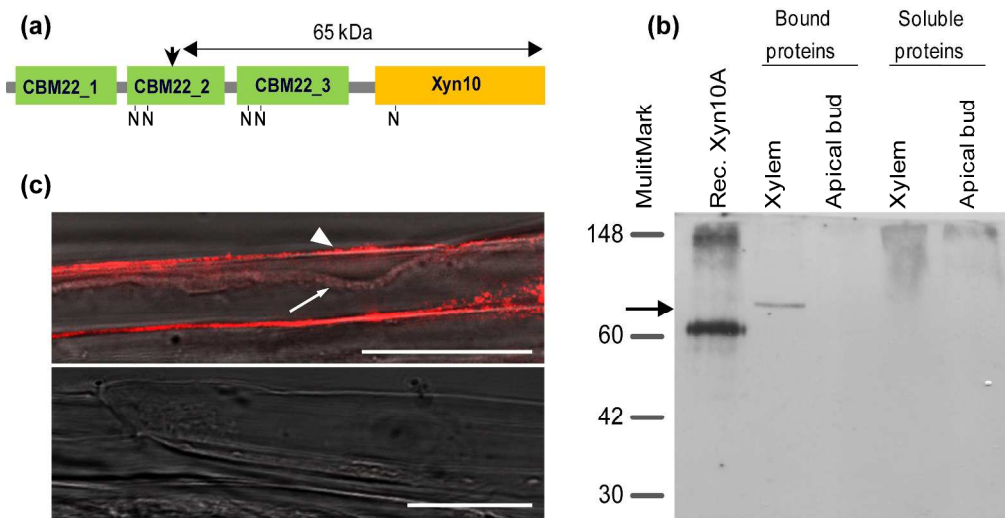
| Line | Ara | Gal | Glc | Xyl | Man | Klason lignin | Acid soluble lignin | Total lignin |
|---|-------|-------|-------|-------|-------|---------------|---------------------|--------------|
| | % | % | % | % | % | % | % | % |
| 2 | 0.32 | 1.15* | 51.6* | 18.8* | 3.01* | 20.9* | 4.20* | 25.1* |
| 3 | 0.35 | 1.08* | 51.5* | 19.7* | 3.07 | 19.8* | 4.43* | 24.3* |
| 32 | 0.32 | 1.17* | 51.8* | 19.3* | 2.94 | 19.9* | 4.45* | 24.4* |
| WT | 0.35 | 1.69 | 54.3 | 18.1 | 2.51 | 19.0 | 4.09 | 23.0 |
| $P_{WT \text{ vs. } Xyn10A \text{ AS}}^1$ | 0.620 | 0.004 | 0.001 | 0.001 | 0.049 | 0.001 | 0.001 | 0.001 |

* $P \leq 5\%$ (*t* test);

¹ $P_{WT \text{ vs. } Xyn10A \text{ AS}}$ values correspond to the difference between all transgenic lines and the WT.

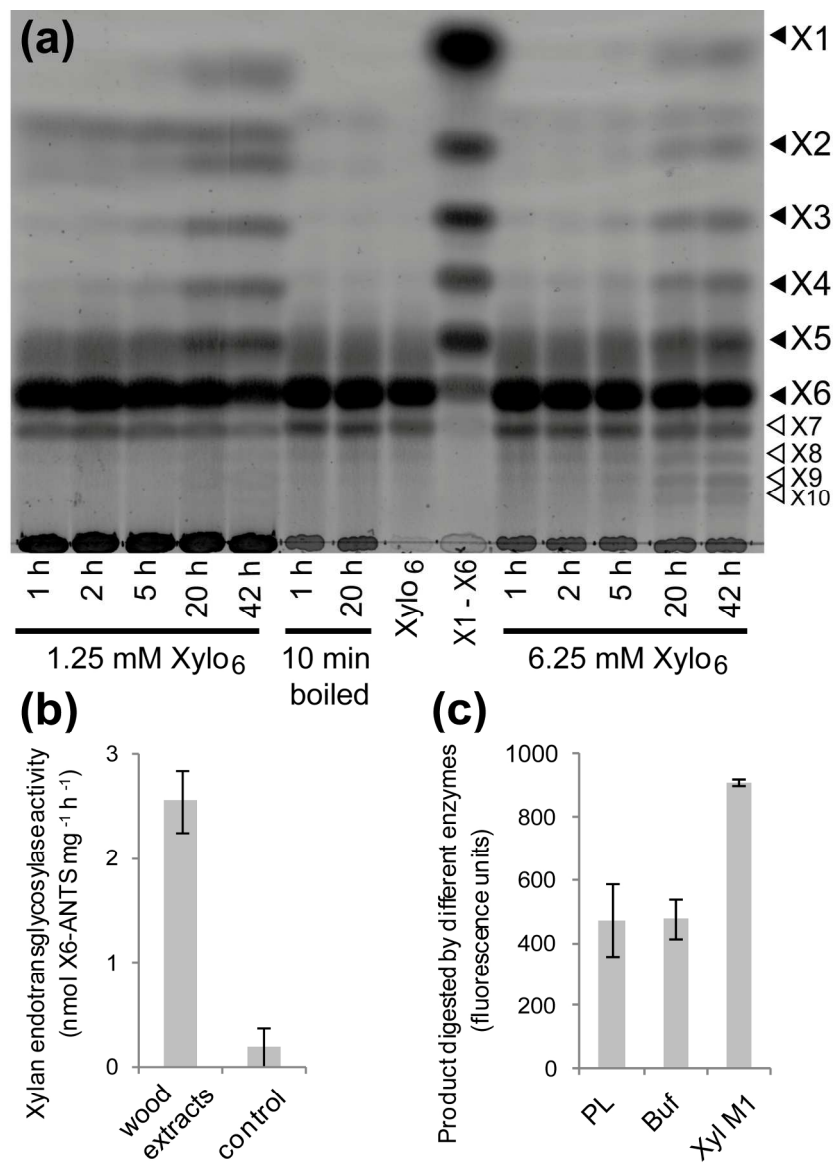
Table 2. Cell wall and stress signalling related transcripts significantly affected in both transgenic antisense lines, 2 and 32, as compared to the WT.

| Class | Gene | Annotation | M value | | Closest <i>A. thaliana</i> |
|----------------------------------|----------------------------------|---|---------|-----------|-------------------------------|
| | | | 2 | 32 | |
| pectins | Potri.014G004500 | Rhamnogalacturonate lyase family protein | -2.487 | -0.880 | AT2G22620 |
| | Potri.010G152000 | polygalacturonase <i>PtGH28_75</i> | 0.749 | 0.895 | AT1G48100 |
| | Potri.003G156600 | similar to GALACTAN SYNTHASE 2 | -2.472 | -0.805 | AT5G44670 |
| | Potri.001G052300 | pectate lyase <i>PtPL1_26</i> | 0.604 | 1.072 | AT4G13710 |
| | Potri.015G087800 | similar to probable pectate lyase 22 | 0.491 | 1.077 | AT5G63180 |
| xylan | Potri.008G108100 | similar to beta-D-xylosidase | 1.049 | 0.841 | AT5G49360 |
| xyloglucan | Potri.018G095100 | <i>PtXTH16_17</i> | -0.835 | -0.884 | AT4G25810 |
| | Potri.017G101300 | O-fucosyltransferase family protein | -1.839 | -0.637 | AT5G15740 |
| mannan | Potri.013G130400 | similar to ENDO-BETA-MANNASE 2 | 1.363 | 1.037 | AT2G20680 |
| AGP | Potri.013G151300 | fasciclin-like AGP <i>PtFLA12K</i> | -2.692 | -1.097 | AT5G60490 |
| | Potri.012G015000 | similar to fasciclin-like FLA 11 | -1.942 | -1.005 | AT5G03170 |
| | Potri.009G012200 | fasciclin-like AGP <i>PtFLA12V</i> | -1.786 | -0.878 | AT5G60490 |
| | Potri.013G151500 | fasciclin-like AGP <i>PtFLA12J</i> | -2.138 | -1.179 | AT5G60490 |
| | Potri.019G123200 | similar to fasciclin-like FLA 11 | -2.187 | -1.157 | AT5G03170 |
| | Potri.015G013300 | fasciclin-like AGP <i>PtFLA12E</i> or <i>F</i> | -2.090 | -1.236 | AT5G03170 |
| | Potri.009G012100 | fasciclin-like AGP <i>PtFLA12G</i> , <i>P</i> or <i>Q</i> | -2.242 | -1.313 | AT5G03170 |
| | Potri.001G450200 | beta-galactosyltransferase <i>PtGT31_32</i> | -1.286 | -0.617 | AT1G32930 |
| | Potri.013G151400 | similar to fasciclin-like FLA 11 | -2.293 | -1.174 | AT5G03170 |
| | Potri.006G144500 | Similar to glycosyl hydrolase family 35 | 0.588 | 0.557 | AT3G13750 |
| Potri.005G161100 | similar to AGP5 | -1.109 | -0.705 | AT1G35230 | |
| cellulose | Potri.002G034000 | Fruktokinase | -2.399 | -0.729 | AT1G19600 |
| | Potri.004G117200 | similar to COBRA like COBL4 | -2.845 | -0.971 | AT5G15630 |
| | Potri.003G151700 | similar to KORRIGAN1 <i>PtCel9A1</i> | -1.436 | -0.727 | AT5G49720 |
| lignin | Potri.008G038200 | phenylalanine ammonia-lyase1 (PAL1) | 1.333 | 0.752 | AT2G37040 |
| | Potri.018G100500 | cinnamoyl-CoA reductase related | 1.147 | 0.598 | AT2G23910 |
| microtubule | Potri.008G139700 | microtubule associated MAP65-like | 1.795 | 1.214 | AT2G01910 |
| | Potri.014G088500 | similar to <i>AtMPK4</i> | 0.745 | 0.783 | AT4G01370 |
| | Potri.006G018000 | similar to <i>AtMAP70-5</i> | 1.443 | 1.383 | AT4G17220 |
| LRK | Potri.008G140500 | Similar to BRL2 | 0.816 | 0.550 | AT2G01950 |
| | Potri.012G128700 | Leucine-rich repeat protein kinase family protein | 0.739 | 0.992 | AT5G51560 |
| | Potri.019G122700 | Leucine-rich repeat receptor-like protein kinase family protein; | -1.469 | -0.556 | AT4G08850 |
| calcium | Potri.001G005500 | Calcium binding protein involved in cryptochrome and phytochrome coaction | 1.624 | 1.495 | AT4G08810 |
| | Potri.016G049100 | CaLB domain, plant phosphoribosyltransferase family protein | 0.861 | 0.858 | AT3G57880 |
| | Potri.009G052700 | similar to calcium-dependent protein kinase 1; MSCK1 | 0.899 | 0.651 | AT5G12480 |
| vesicle | Potri.001G278800 | clathrin heavy chain | 2.885 | 2.942 | AT3G11130 |
| ethylene, stress | Potri.017G108800 | similar to S-adenosylmethionine decarboxylase. | -2.343 | -1.119 | AT3G02470 |
| | Potri.013G044100 | ethylene receptor EIN4-like | 1.184 | 1.134 | AT3G04580 |
| | Potri.014G159000 | similar to ACC oxidase | -1.038 | -1.225 | AT1G05010 |
| | Potri.002G078600 | similar to ACC oxidase | -2.125 | -1.168 | AT1G77330 |
| | Potri.004G003000 | similar to ACC oxidase | -1.193 | -0.706 | AT1G05010 |

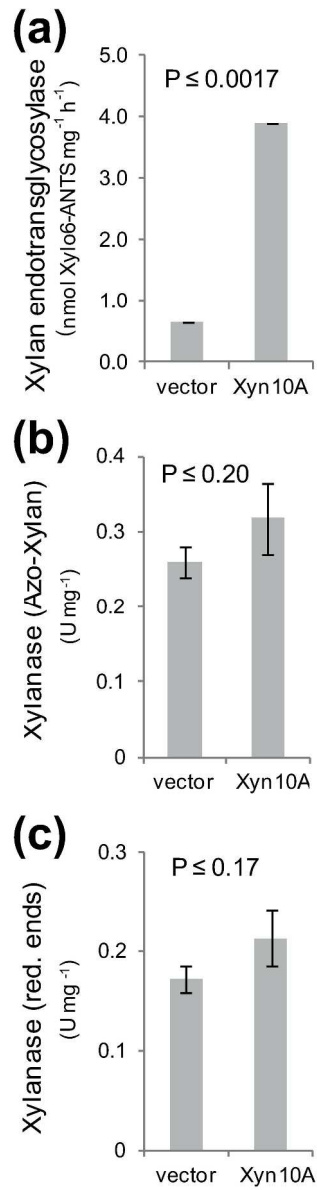


330x169mm (300 x 300 DPI)

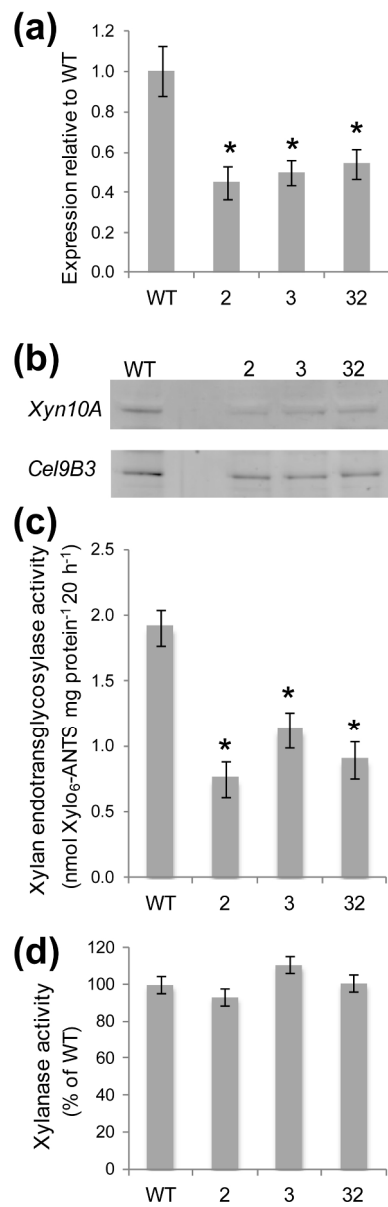
Peer Review



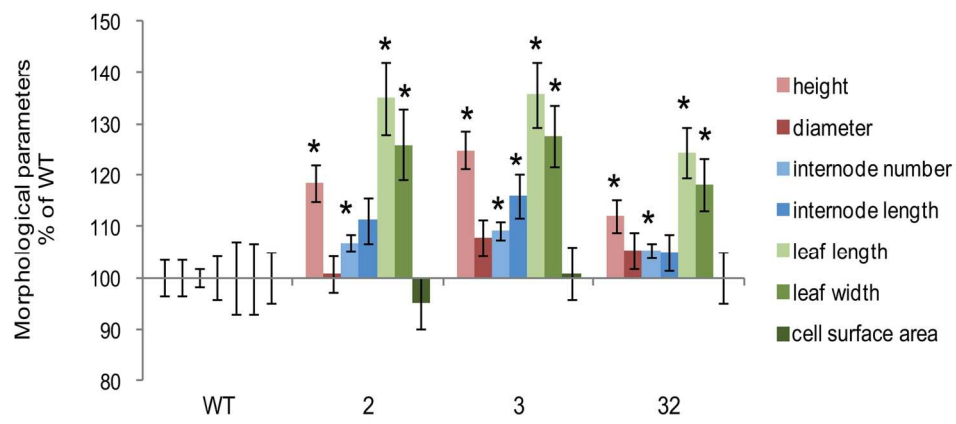
157x226mm (300 x 300 DPI)



221x748mm (300 x 300 DPI)

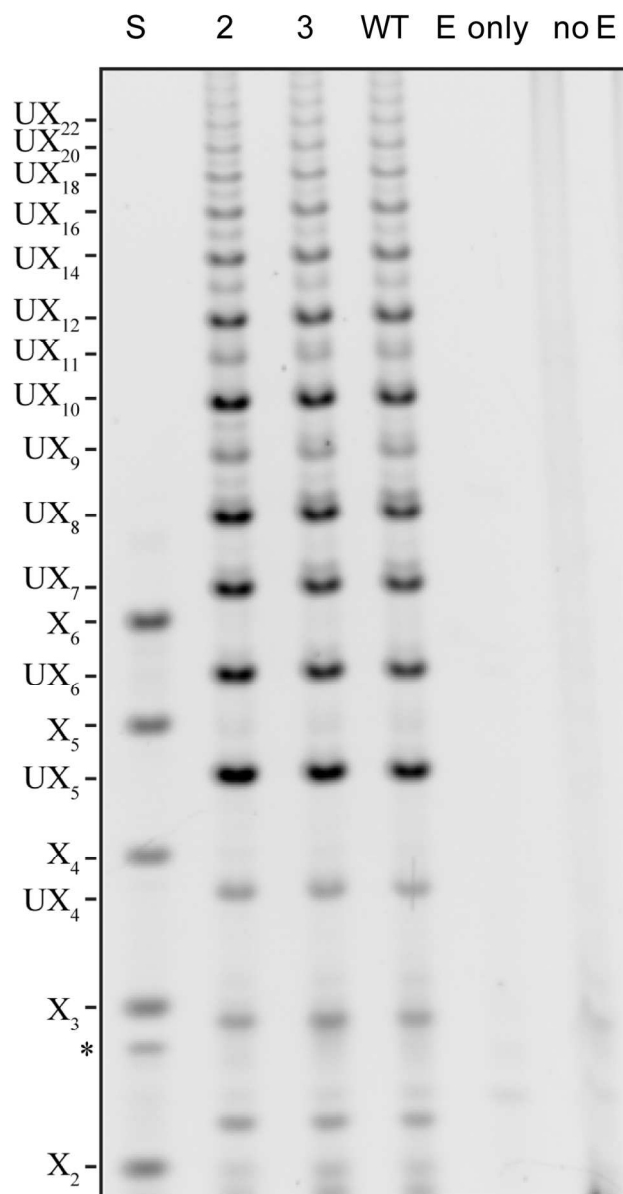


99x273mm (300 x 300 DPI)

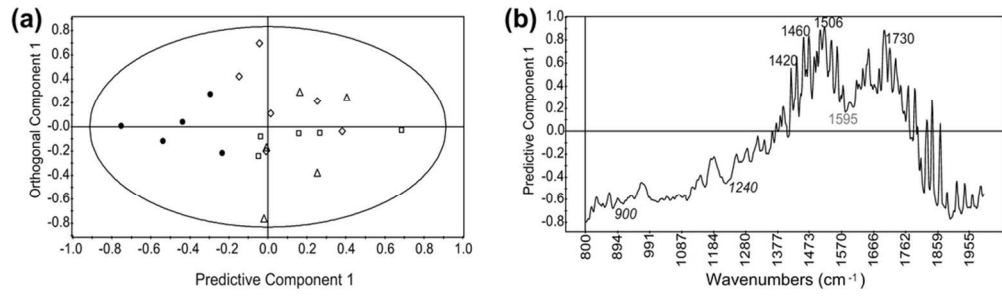


149x66mm (300 x 300 DPI)

Peer Review

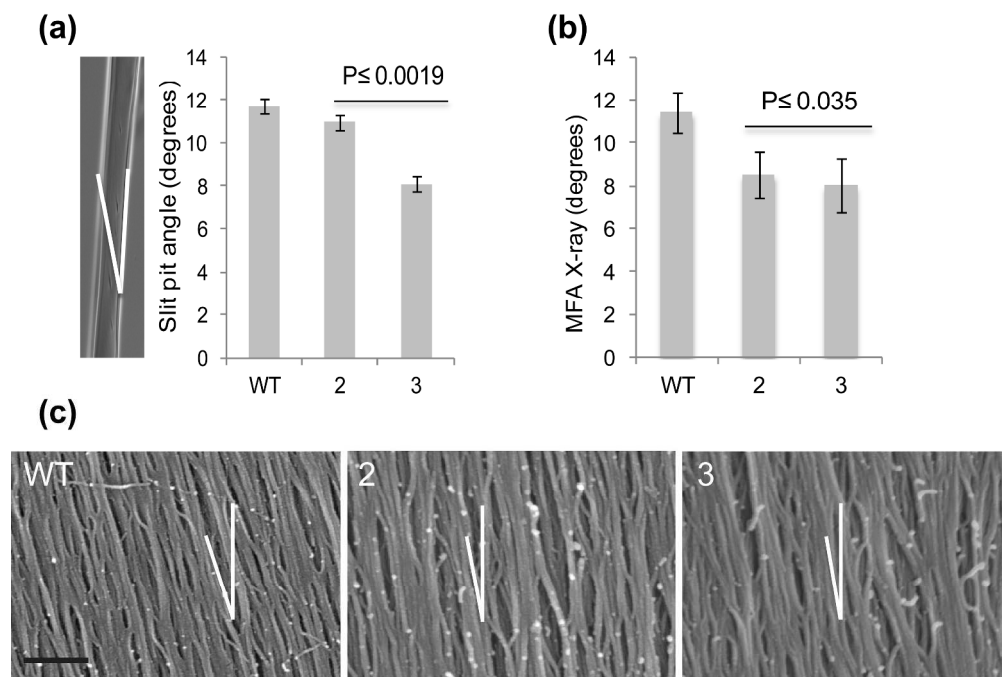


95x184mm (300 x 300 DPI)



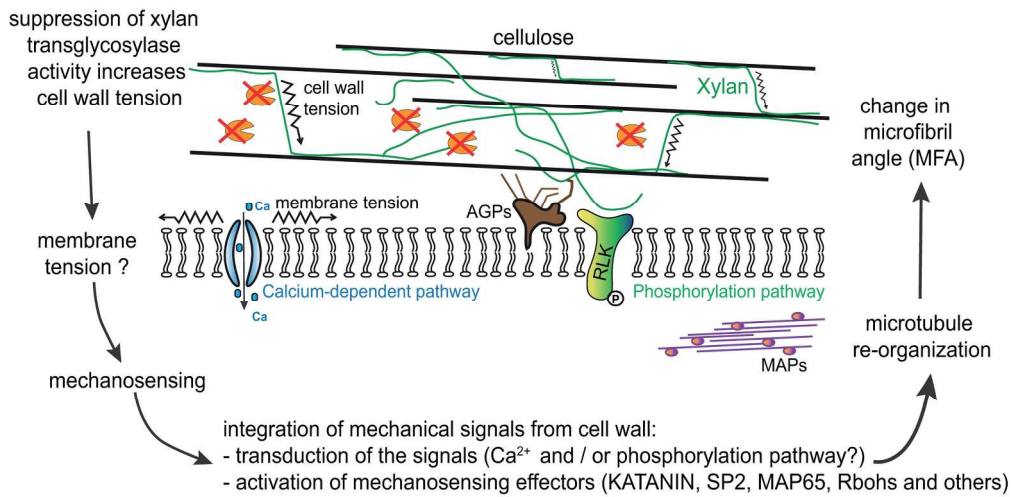
92x26mm (300 x 300 DPI)

For Peer Review



261x175mm (300 x 300 DPI)

Review



189x92mm (300 x 300 DPI)